The gut microbiome regulates memory function

Emily E Noble[1], Elizabeth Davis[2], Linda Tsan[2], Yen-Wei Chen[3], Christine A. Olson[3], Ruth Schade[1], Clarissa Liu[2], Andrea Suarez[2], Roshonda B Jones[2], Michael I Goran[2], Claire de La Serre[1], Xia Yang[3], Elaine Y. Hsiao[3], and Scott E Kanoski[2]

[1]University of Georgia, Athens, Georgia, USA; [2]University of Southern California, Los Angeles, California, USA; [3]University of California, Los Angeles, California, USA

Correspondence:
Scott E. Kanoski, Ph.D
University of Southern California
3616 Trousdale Parkway, AHF-252
Los Angeles, CA 90089-0372
Phone: 213-821-5762
Email: kanoski@usc.edu

Key Words: sugar-sweetened beverages, hippocampus, adolescence, bacteria, juvenile, brain, microbiota, early-life, development, learning and memory

Abstract (250 words)

The mammalian gastrointestinal tract contains a diverse ecosystem of microbial species collectively making up the gut microbiota. Emerging evidence highlights a critical relationship between gut microbiota and neurocognitive development. Consumption of unhealthy yet palatable dietary factors associated with obesity and metabolic dysfunction (e.g., saturated fat, added sugar) alters the gut microbiota and negatively impacts neurocognitive function, particularly when consumed during early life developmental periods. Here we explore whether excessive early life consumption of added sugars negatively impacts neurocognitive development via the gut microbiome. Using a rodent model of habitual sugar-sweetened beverage (SSB) consumption during the adolescent stage of development, we first show that excessive early life sugar intake impairs hippocampal-dependent memory function when tested during adulthood while preserving other neurocognitive domains. 16S rRNA gene sequencing of the fecal and cecal microbiota reveals that early life SSB consumption alters the relative abundance of various bacterial taxa. In particular, SSB elevates fecal operational taxonomic units within the genus *Parabacteroides,* which negatively correlate with memory task performance. Additional results reveal that transferred enrichment of *Parabacteroides* species *P. distasonis* and *P. johnsonii* in adolescent rats impairs memory function during adulthood. Hippocampus transcriptome analyses identify gene expression alterations in neurotransmitter synaptic signaling, intracellular kinase signaling, metabolic function, neurodegenerative disease, and dopaminergic synaptic signaling-associated pathways as potential mechanisms linking bacterial alterations with memory impairment. Collectively these results identify a role for microbiota “dysbiosis” in

48 mediating the negative effects of early life unhealthy dietary factors on neurocognitive
49 outcomes.
50

Introduction

The gut microbiome is increasingly implicated in modulating neurocognitive development and consequent functioning [1,2]. Early life developmental periods represent critical windows for the impact of indigenous gut microbes on the brain, as evidenced by the reversal of behavioral and neurochemical abnormalities in germ free rodents when inoculated with conventional microbiota during early life, but not during adulthood [3-5]. Dietary factors are a critical determinant of gut microbiota diversity and can alter gut bacterial communities, as evident from the microbial plasticity observed in response to pre- and probiotic treatment, as well as the "dysbiosis" resulting from consuming unhealthy, yet palatable foods that are associated with obesity and metabolic disorders (e.g., "Western diet"; foods high in saturated fatty acids and added sugar) [6]. In addition to altering the gut microbiota, consumption of these dietary factors yields long-lasting memory impairments, and these effects are more pronounced when consumed during early life developmental periods vs. during adulthood [7-9]. Whether diet-induced changes in specific bacterial populations are functionally related to altered early life neurocognitive outcomes, however, is poorly understood.

The hippocampus, which is well known for its role in spatial and episodic memory and more recently for regulating learned and social aspects of food intake control [10-15], is particularly vulnerable to the deleterious effects of Western dietary factors [16-18]. During the juvenile and adolescent stages of development, a time when the brain is rapidly developing, consumption of diets high in saturated fat and sugar [19-21] or sugar alone [22-25] impairs hippocampal function while in some cases preserving memory processes that do

not rely on the hippocampus. While several putative underlying mechanisms have been investigated, the precise biological pathways linking dietary factors to neurocognitive dysfunction remain largely undetermined [9]. Here we aimed to determine whether sugar-induced alterations in gut microbiota during early life are causally related to hippocampal-dependent memory impairments observed during adulthood.

Early-life sugar consumption impairs hippocampal-dependent memory function without affecting other neurocognitive domains

Results from the Novel Object in Context (NOIC) task, which measures hippocampal-dependent episodic contextual memory function [26], reveal that while there were no differences in total exploration time of the combined objects on days 1 or 3 of the task (Fig. 1A,B), animals fed sugar solutions in early life beginning at PN 28 had a reduced capacity to discriminate an object that was novel to a specific context when animals were tested during adulthood (PN 60), indicating impaired hippocampal function (Fig. 1C, D). Conversely, when tested in the novel object recognition task (NOR), which tests object recognition memory independent of context and is primarily dependent on the perirhinal cortex [26-28], animals fed sugar solutions in early life performed similarly to those in the control group (Fig. 1E).

Elevated anxiety and altered general activity levels may influence novelty exploration independent of memory effects and may therefore confound the interpretation of behavioral results. Thus, we next tested whether early life sugar consumption affects anxiety-like behavior using two different tasks designed to measure anxiety in the rat:

the elevated zero maze and the open field task, that latter of which also assesses levels of general activity [29]. Early life sugar had no effect on time spent in the open area or in the number of open area entries in the zero maze (Fig. 1F, G). Similarly, early life sugar had no effect on distance travelled or time spent in the center zone in the open field task (Fig. 1H, I). Together these data suggest that habitual early life sugar consumption did not increase anxiety-like behavior or general activity levels in the rats.

Early life sugar consumption impairs glucose tolerance without affecting total caloric intake, body weight, or adiposity

Given that excessive sugar consumption is associated with weight gain and metabolic deficits [30], we tested whether access to a sugar solution during the adolescent phase of development would affect food intake, body weight gain, adiposity, and glucose tolerance in the rat. Early life sugar consumption had no effect on body weight or total kcal intake (Fig. 1J, K), which is in agreement with previous findings [22,31,32]. Animals steadily increased their intake of the 11% sugar solution throughout the study but compensated for the calories consumed in the sugar solutions by reducing their intake of dietary chow (Supplemental Fig. 1A, B). There were no differences in body fat percentage during adulthood (Fig. 1L) or in total grams of body fat or lean mass. However, animals that were fed sugar solutions during early life showed impaired peripheral glucose metabolism in an intraperitoneal glucose tolerance test (IP GTT) (Fig. 1L, Supplemental Fig 1C-E).

Gut microbiota are impacted by early life sugar consumption

Principal component analyses of 16s rRNA gene sequencing data of fecal samples revealed a separation between the fecal microbiota of rats fed early life sugar and controls (Fig. 2A). Results from LEfSe analysis identified differentially abundant bacterial taxa in fecal samples that were elevated by sugar consumption. These include the family *Clostridiaceae* and the genus *02d06* within *Clostridiaceae*, the family *Mogibacteriaceae*, the family *Enterobacteriaceae*, the order *Enterobacteriales*, the class of *Gammaproteobacteria*, and the genus *Parabacteroides* within the family *Porphyromonadaceae* (Fig. 2B,C). In addition to an elevated % relative abundance of the genus *Parabacteroides* in animals fed early life sugar (Fig 2D), log transformed counts of the *Parabacteroides* negatively correlated with performance scores in the NOIC memory task (R^2=.64, P<.0001; Fig. 2E). Within *Parabacteroides*, levels of three operational taxonomic units (OTUs) that were elevated by sugar significantly correlated negatively with performance in the NOIC task, two of which were identified as taxonomically related to *P. johnsonii* and *P. distasonis* (Fig. 2F, G). The significant negative correlation between NOIC performance and each of these OTUs was also present within the sugar groups alone (not shown). Abundance of other bacterial populations that were affected by sugar consumption were not significantly related to memory task performance.

There was a similar separation between groups in bacteria analyzed from cecal samples (Supplemental Fig. 2A). LEfSe results from cecal samples show elevated *Bacilli*, *Actinobacteria*, *Erysipelotrichia*, and *Gammaproteobacteria* in rats fed early life sugar, and elevated *Clostridia* in the controls (Supplemental Fig. 2B). Abundances at the different taxonomic levels in fecal and cecal samples are shown in (Supplemental Fig. 3,

4). Regression analyses did not identify these altered cecal bacterial populations as being significantly correlated to NOIC memory performance.

Early life *Parabacteroides* enrichment impairs memory function

To determine whether neurocognitive outcomes due to early life sugar consumption could be attributable to elevated levels of *Parabacteroides* in the gut, we experimentally enriched the gut microbiota of naïve juvenile rats with two *Parabacteroides* species that exhibited high 16S rRNA sequencing alignment with OTUs that were increased by sugar consumption and were negatively correlated with behavioral outcomes in rats fed early life sugar. *P. johnsonii* and *P. distasoni* species were cultured individually under anaerobic conditions and transferred to a group of antibiotic-treated young rats in a 1:1 ratio via oral gavage using the experimental design described in Methods and outlined in Supplemental Fig. 5A, and from [33]. All rats treated with antibiotics showed a reduction in food intake and body weight during the initial stages of antibiotic treatment, however, there were no differences in body weight between the two groups of antibiotic treated animals by PN50, at the time of testing (Supplemental Fig. 5B, C).

Results from the hippocampal-dependent NOIC memory task showed that while there were no differences in total exploration time of the combined objects on days 1 or 3 of the task, indicating similar exploratory behavior, animals treated with *Parabacteroides* showed a significantly reduced discrimination index in the NOIC task (Fig 3A-D), indicating impaired performance in hippocampal-dependent memory function. When tested in the perirhinal cortex-dependent NOR task [26], animals treated with *Parabacteroides* showed impaired object recognition memory as indicated by a

reduced novel object exploration index, with no differences in total exploration time (Fig 3E). These findings show that unlike sugar-fed animals, *Parabacteroides* enrichment impaired perirhinal cortex-dependent memory processes in addition to hippocampal-dependent memory.

Results from the zero maze showed a non-significant trend toward reduced time spent in the open arms and a reduced number of open arm entries for the *Parabacteroides* treated rats (Fig 3F, G), which is indicative of increased anxiety-like behavior. However, there were no differences in distance travelled or time spent in the center arena in the open field test, which is a measure of both anxiety-like behavior and general activity in rodents (Fig. 3H, I). Together these data suggest that *Parabacteroides* treatment negatively impacted both hippocampal-dependent perirhinal cortex-dependent memory function without significantly affecting general activity or anxiety-like behavior.

Similar to a recent report [34], *Parabacteroides* enrichment in the present study impacted body weight. Animals who received *P. johnsonii* and *P. distasonis* treatment showed reduced body weight 40 days after the transfer, with significantly lower lean mass and a trend toward reduced fat mass (Fig 3J-L). There were no differences in percent body fat between groups, nor were there significant group differences in glucose metabolism in the IPGTT (Supplemental Fig. 5D, E).

Early life sugar consumption and *Parabacteroides* enrichment alter hippocampal gene expression profiles

194 To further investigate how sugar and *Parabacteroides* affect cognitive behaviors, we
195 conducted transcriptome analysis of the hippocampus samples. Supplemental Fig 6A
196 shows the results of principal component analysis revealing moderate separation based
197 on RNA sequencing data from the dorsal hippocampus of rats fed sugar in early life
198 compared with controls. Gene pathway enrichment analyses from RNA sequencing data
199 revealed multiple pathways significantly affected by early life sugar consumption,
200 including four pathways involved in neurotransmitter synaptic signaling: dopaminergic,
201 glutamatergic, cholinergic, and serotonergic signaling pathways. Additionally, several
202 gene pathways that also varied by sugar were those involved in kinase-mediated
203 intracellular signaling: cGMP-PKG, RAS, cAMP, and MAPK signaling pathways (Fig. 4A,
204 Supplemental Table 1).

205 Analyses of individual genes across the entire transcriptome using a stringent
206 false-discovery rate criterion further identified 21 genes that were differentially
207 expressed in rats fed early life sugar compared with controls, with 11 genes elevated and
208 10 genes decreased in rats fed sugar compared to controls (Fig 4B). Among the genes
209 impacted, several genes that regulate cell survival, migration, differentiation, and DNA
210 repair were elevated by early life sugar access, including *Faap100*, which encodes an FA
211 core complex member of the DNA damage response pathway [35], and *Eepd1*, which
212 transcribes an endonuclease involved in repairing stalled DNA replication forks,
213 stressed from DNA damage [36]. Other genes associated with ER stress and
214 synaptogenesis were also significantly increased by sugar consumption, including *Klf9,*
215 *Dgkh, Neurod2, Ppl*, and *Kirrel1* [37,38,39,40].

216 Several genes were reduced by dietary sugar, including *Tns2*, which encodes
217 tensin 2, important for cell migration [41], *RelA*, which encodes a NF/kB complex protein

that regulates activity dependent neuronal function and synaptic plasticity [42], and *Grm8*, the gene for the metabotropic glutamate receptor 8 (mGluR8). Notably, reduced expression of mGluR8 receptor may contribute to the impaired neurocognitive functioning in animals fed sugar, as mGluR8 knockout mice show impaired hippocampal-dependent learning and memory [43].

Supplemental Fig 6B shows the results of principal component analysis of dorsal hippocampus RNA sequencing data indicating moderate separation between rats enriched with *Parabacteroides* and controls. Gene pathway analyses revealed that early life *Parabacteroides* treatment, similar to effects associated with sugar consumption, significantly altered the genetic signature of dopaminergic synaptic signaling pathways, though differentially expressed genes were commonly affected in opposite directions between the two experimental conditions (Supplemental Fig 7). *Parabacteroides* treatment also impacted gene pathways associated with metabolic signaling. Specifically, pathways regulating fatty acid oxidation, rRNA metabolic processes, mitochondrial inner membrane, and valine, leucine, and isoleucine degradation were significantly affected by *Parabacteroides* enrichment. Other pathways that were influenced were those involved in neurodegenerative disorders, including Alzheimer's disease and Parkinson's disease, though most of the genes affected in these pathways were mitochondrial genes (Fig. 4D, Supplemental Table 2).

At the level of individual genes, dorsal hippocampal RNA sequencing data revealed that 15 genes were differentially expressed in rats enriched with *Parabacteroides* compared with controls, with 13 genes elevated and two genes decreased in the *Parabacteroides* group compared with controls (Fig 4C). Consistent with results from gene pathway analyses, several individual genes involved in metabolic

processes were elevated by *Parabacteroides* enrichment, such as *Hmgcs2*, which is a mitochondrial regulator of ketogenesis and provides energy to the brain under metabolically taxing conditions or when glucose availability is low [44], and *Cox6b1*, a mitochondrial regulator of energy metabolism that improves hippocampal cellular viability following ischemia/reperfusion injury [45]. *Parabacteroides* enrichment was also associated with incased expression of *Slc27A1* and *Mfrp*, which are each critical for the transport of fatty acids into the brain across capillary endothelial cells [46,47].

Discussion

Dietary factors are a key source of gut microbiome diversity [31,33,48-50] and emerging evidence indicates that diet-induced alterations in the gut microbiota may be linked with altered neurocognitive development [33,50-52]. Our results identify species within the genus *Parabacteroides* that are elevated by habitual early life consumption of dietary sugar and are negatively associated with hippocampal-dependent memory performance. Further, targeted microbiota enrichment of *Parabacteroides* perturbed both hippocampal- and perirhinal cortex-dependent memory performance. These findings are consistent with previous literature in showing that early life consumption of Western dietary factors impair neurocognitive outcomes [8,9], and further suggest that altered gut bacteria due to excessive early life sugar consumption may functionally link dietary patterns with cognitive impairment.

Our previous data show that rats are not susceptible to habitual sugar consumption-induced learning and memory impairments when 11% sugar solutions are consumed ad libitum during adulthood, in contrast to effects observed in the present and previous study in which the sugar is consumed during early life development [22]. It is

possible that habitual sugar consumption differentially affects the gut microbiome when consumed during adolescence vs. adulthood. However, a recent report showed that adult consumption of a high fructose diet (35% kcal from fructose) promotes gut microbial "dysbiosis" and neuroinflammation and cell death in the hippocampus, yet without impacting cognitive function [53], suggesting that perhaps neurocognitive function is more susceptible to gut microbiota influences during early life than during adulthood. Indeed, several reports have identified early life critical periods for microbiota influences on behavioral and neurochemical endpoints in germ free mice [3,5,4]. However, the age-specific profile of sugar-associated microbiome dysbiosis and neurocognitive impairments remains to be determined.

While our study reveals a strong negative correlation between levels of fecal *Parabacteroides* and performance in the hippocampal-dependent contextual episodic memory NOIC task, as well as impaired NOIC performance in rats given access to a sugar solution during adolescence, sugar intake did not produce impairments in the perirhinal cortex-dependent NOR memory task. That early life sugar consumption negatively impacts hippocampal-dependent spatial [22] and contextual-based learning without influencing NOR performance is consistent with previous reports using a cafeteria diet high in both fat content and sugar [54]. On the other hand, enrichment of *P. johnsonii* and *P. distasonis* in the present study impaired memory performance in both tasks, suggesting a broader impact on neurocognitive functioning with this targeted bacterial enrichment approach.

Gene pathway enrichment analyses from dorsal hippocampus RNA sequencing identified multiple neurobiological pathways that may functionally connect gut dysbiosis with memory impairment. Early life sugar consumption was associated with

290 alterations in several neurotransmitter synaptic signaling pathways (e.g., glutamatergic,
291 cholinergic) and intracellular signaling targets (e.g., cAMP, MAPK). A different profile
292 was observed in *Parabacteroides*-enriched animals, where gene pathways involved with
293 metabolic function (e.g., fatty acid oxidation, branched chain amino acid degradation)
294 and neurodegenerative disease (e.g., Alzheimer's disease) were altered relative to
295 controls. Given that sugar has effects on bacterial populations in addition to
296 *Parabacteroides*, and that sugar consumption and *Parabacteroides* treatment
297 differentially influenced peripheral glucose metabolism and body weight, these
298 transcriptome differences in the hippocampus are not surprising. However, gene
299 clusters involved with dopaminergic synaptic signaling were significantly influenced by
300 both early life sugar consumption and *Parabacteroides* treatment, thus identifying a
301 common pathway through which both diet-induced and gut bacterial infusion-based
302 elevations in *Parabacteroides* may influence neurocognitive development. Though
303 differentially expressed genes were commonly affected in opposite directions in
304 *Parabacteroides* enriched animals compared with early life sugar treated animals, it is
305 possible that perturbations to the dopamine system play a role in the observed cognitive
306 dysfunction. For example, while dopamine signaling in the hippocampus has not
307 traditionally been investigated for mediating memory processes, several recent reports
308 have identified a role for dopamine inputs from the locus coeruleus in regulating
309 hippocampal-dependent memory and neuronal activity [55,56]. Interestingly, endogenous
310 dopamine signaling in the hippocampus has recently been linked with regulating food
311 intake and food-associated contextual learning [57], suggesting that dietary effects on gut
312 microbiota may also impact feeding behavior and energy balance-relevant cognitive
313 processes.

Many of the genes that were differentially upregulated in the hippocampus by *Parabacteroides* enrichment were involved in fat metabolism and transport. Thus, it is possible that *Parabacteroides* conferred an adaptation in the brain, shifting fuel preference away from carbohydrate toward lipid-derived ketones. Consistent with this framework, *Parabacteroides* was previously shown to be upregulated by a ketogenic diet in which carbohydrate consumption is drastically depleted and fat is used as a primary fuel source due. Furthermore, enrichment of *Parabacteroides merdae* together with *Akkermansia muciniphila* was protective against seizures in mice [33]. It is possible that *P. distasonis* reduces glucose uptake from the gut, enhances glucose clearing from the blood, and/or alter nutrient utilization in general, an idea further supported by recent finding that *P. distasonis* is associated with reduced diet- and genetic-induced obesity and hyperglycemia in mice [34].

Collective results provide mechanistic insight into the neurobiological mechanisms that link early life unhealthy dietary patters with altered gut microbiota changes and neurocognitive impairments. Currently probiotics, live microorganisms intended to confer health benefits, are not regulated with the same rigor as pharmaceuticals but instead are sold as dietary supplements. Our findings suggest that gut enrichment with certain species of *Parabacteroides* is potentially harmful for neurocognitive mnemonic development. These results highlight the importance of conducting rigorous basic science analyses on the relationship between diet, microorganisms, brain, and behavior prior to widespread recommendations of bacterial microbiome interventions for humans.

Acknowledgements

We thank Alyssa Cortella for contributing the rodent artwork. We thank Caroline Szjewski, Lekha Chirala, Vaibhav Konanur, Sarah Terrill, and Ted Hsu for their critical contributions to the research. The research was supported by DK104897, DK118402, and institutional funds to S.E.K., DK111158 to E.E.N., DK116558 to A.N.S., DK 118944 to C.M.L. C.A.O. was supported by an F31 AG064844. E.Y.H. was supported by ARO MURI award W911NF-17-1-0402. DK104363 to X.Y., Eureka Scholarship and BWF-CHIP Fellowship to Y.C.

Author Contributions

E.E.N. and S.E.K. designed the experiments. E.E.N. performed the majority of the behavioral experiments and analyzed the data. E.D. helped with the behavioral experiments and performed the RNA sequencing preparation with Y.C. and X.Y. for analyses of the RNA sequencing data. C.A.O. and E.Y.H. contributed to the design and implementation of the bacterial enrichment procedure. R.J., M.G., R. S. and C.D.L.S., performed the gut microbiome analyses. L.T., C.L., and A.S., helped with behavioral experiments. The paper was written by E.E.N and S.E.K. with additional editorial input from the other authors.

Competing interests

The authors declare no competing interests

References

1 Vuong, H. E., Yano, J. M., Fung, T. C. & Hsiao, E. Y. The Microbiome and Host Behavior. *Annu Rev Neurosci* **40**, 21-49, doi:10.1146/annurev-neuro-072116-031347 (2017).

2 Noble, E. E., Hsu, T. M. & Kanoski, S. E. Gut to Brain Dysbiosis: Mechanisms Linking Western Diet Consumption, the Microbiome, and Cognitive Impairment. *Frontiers in behavioral neuroscience* **11**, 9, doi:10.3389/fnbeh.2017.00009 (2017).

3 Neufeld, K. A., Kang, N., Bienenstock, J. & Foster, J. A. Effects of intestinal microbiota on anxiety-like behavior. *Commun Integr Biol* **4**, 492-494, doi:10.4161/cib.4.4.15702 (2011).

4 Sudo, N. *et al.* Postnatal microbial colonization programs the hypothalamic-pituitary-adrenal system for stress response in mice. *J Physiol* **558**, 263-275, doi:10.1113/jphysiol.2004.063388 (2004).

5 Diaz Heijtz, R. *et al.* Normal gut microbiota modulates brain development and behavior. *Proc Natl Acad Sci U S A* **108**, 3047-3052, doi:10.1073/pnas.1010529108 (2011).

6 Cryan, J. F. *et al.* The Microbiota-Gut-Brain Axis. *Physiological reviews* **99**, 1877-2013, doi:10.1152/physrev.00018.2018 (2019).

7 Kanoski, S. E. & Davidson, T. L. Western diet consumption and cognitive impairment: links to hippocampal dysfunction and obesity. *Physiol Behav* **103**, 59-68, doi:10.1016/j.physbeh.2010.12.003 (2011).

8 Noble, E. E., Hsu, T. M., Liang, J. & Kanoski, S. E. Early-life sugar consumption has long-term negative effects on memory function in male rats. *Nutritional neuroscience*, 1-11, doi:10.1080/1028415X.2017.1378851 (2019).

9 Noble, E. E. & Kanoski, S. E. Early life exposure to obesogenic diets and learning and memory dysfunction. *Curr Opin Behav Sci* **9**, 7-14, doi:10.1016/j.cobeha.2015.11.014 (2016).

10 Hsu, T. M. *et al.* Hippocampus ghrelin receptor signaling promotes socially-mediated learned food preference. *Neuropharmacology* **131**, 487-496, doi:10.1016/j.neuropharm.2017.11.039 (2018).

11 Hsu, T. M. *et al.* A hippocampus to prefrontal cortex neural pathway inhibits food motivation through glucagon-like peptide-1 signaling. *Mol Psychiatry* **23**, 1555-1565, doi:10.1038/mp.2017.91 (2018).

12 Hsu, T. M. *et al.* Hippocampus ghrelin signaling mediates appetite through lateral hypothalamic orexin pathways. *Elife* **4**, doi:10.7554/eLife.11190 (2015).

13 Kanoski, S. E., Fortin, S. M., Ricks, K. M. & Grill, H. J. Ghrelin Signaling in the Ventral Hippocampus Stimulates Learned and Motivational Aspects of Feeding via PI3K-Akt Signaling. *Biol Psychiatry* **73**, 915-923, doi:10.1016/j.biopsych.2012.07.002 (2013).

14 Davidson, T. L. *et al.* Contributions of the hippocampus and medial prefrontal cortex to energy and body weight regulation. *Hippocampus* **19**, 235-252, doi:10.1002/hipo.20499 (2009).

15 Kanoski, S. E. & Grill, H. J. Hippocampus Contributions to Food Intake Control: Mnemonic, Neuroanatomical, and Endocrine Mechanisms. *Biol Psychiatry* **81**, 748-756, doi:10.1016/j.biopsych.2015.09.011 (2017).

16 Kanoski, S. E. & Davidson, T. L. Western diet consumption and cognitive impairment: links to hippocampal dysfunction and obesity. *Physiol Behav* **103**, 59-68, doi:10.1016/j.physbeh.2010.12.003 (2011).

17 Davidson, T. L., Sample, C. H. & Swithers, S. E. An application of Pavlovian principles to the problems of obesity and cognitive decline. *Neurobiology of learning and memory* **108**, 172-184, doi:10.1016/j.nlm.2013.07.014 (2014).

18 Baym, C. L. *et al.* Dietary lipids are differentially associated with hippocampal-dependent relational memory in prepubescent children. *Am J Clin Nutr* **99**, 1026-1032, doi:10.3945/ajcn.113.079624 (2014).

19 Valladolid-Acebes, I. *et al.* Spatial memory impairment and changes in hippocampal morphology are triggered by high-fat diets in adolescent mice. Is there a role of leptin? *Neurobiol Learn Mem* **106**, 18-25, doi:10.1016/j.nlm.2013.06.012 (2013).

20 Boitard, C. *et al.* Impairment of hippocampal-dependent memory induced by juvenile high-fat diet intake is associated with enhanced hippocampal inflammation in rats. *Brain Behav Immun* **40**, 9-17, doi:10.1016/j.bbi.2014.03.005 (2014).

21 Boitard, C. *et al.* Juvenile, but not adult exposure to high-fat diet impairs relational memory and hippocampal neurogenesis in mice. *Hippocampus* **22**, 2095-2100, doi:10.1002/hipo.22032 (2012).

22 Hsu, T. M. *et al.* Effects of sucrose and high fructose corn syrup consumption on spatial memory function and hippocampal neuroinflammation in adolescent rats. *Hippocampus* **25**, 227-239, doi:10.1002/hipo.22368 (2015).

23 Kendig, M. D., Boakes, R. A., Rooney, K. B. & Corbit, L. H. Chronic restricted access to 10% sucrose solution in adolescent and young adult rats impairs spatial memory and alters sensitivity to outcome devaluation. *Physiol Behav* **120**, 164-172, doi:10.1016/j.physbeh.2013.08.012 (2013).

24 Reichelt, A. C., Killcross, S., Hambly, L. D., Morris, M. J. & Westbrook, R. F. Impact of adolescent sucrose access on cognitive control, recognition memory, and parvalbumin immunoreactivity. *Learn Mem* **22**, 215-224, doi:10.1101/lm.038000.114 (2015).

25 Noble, E. E., Hsu, T. M., Liang, J. & Kanoski, S. E. Early-life sugar consumption has long-term negative effects on memory function in male rats. *Nutr Neurosci* **22**, 273-283, doi:10.1080/1028415X.2017.1378851 (2019).

26 Balderas, I. *et al.* The consolidation of object and context recognition memory involve different regions of the temporal lobe. *Learn Mem* **15**, 618-624, doi:10.1101/lm.1028008 (2008).

27 Aggleton, J. P. & Brown, M. W. Contrasting hippocampal and perirhinal cortex function using immediate early gene imaging. *Q J Exp Psychol B* **58**, 218-233, doi:10.1080/02724990444000131 (2005).

28 Albasser, M. M., Davies, M., Futter, J. E. & Aggleton, J. P. Magnitude of the object recognition deficit associated with perirhinal cortex damage in rats: Effects of varying the lesion extent and the duration of the sample period. *Behav Neurosci* **123**, 115-124, doi:10.1037/a0013829 (2009).

29 Sestakova, N., Puzserova, A., Kluknavsky, M. & Bernatova, I. Determination of motor activity and anxiety-related behaviour in rodents: methodological aspects and role of nitric oxide. *Interdiscip Toxicol* **6**, 126-135, doi:10.2478/intox-2013-0020 (2013).

30 Goran, M. I. *et al.* The obesogenic effect of high fructose exposure during early development. *Nat Rev Endocrinol* **9**, 494-500, doi:10.1038/nrendo.2013.108 (2013).
31 Noble, E. E. *et al.* Early-Life Sugar Consumption Affects the Rat Microbiome Independently of Obesity. *J Nutr* **147**, 20-28, doi:10.3945/jn.116.238816 (2017).
32 Noble, E. E., Hsu, T. M., Liang, J. & Kanoski, S. E. Early-life sugar consumption has long-term negative effects on memory function in male rats. *Nutr Neurosci*, 1-11, doi:10.1080/1028415X.2017.1378851 (2017).
33 Olson, C. A. *et al.* The Gut Microbiota Mediates the Anti-Seizure Effects of the Ketogenic Diet. *Cell* **173**, 1728-1741 e1713, doi:10.1016/j.cell.2018.04.027 (2018).
34 Wang, K. *et al.* Parabacteroides distasonis Alleviates Obesity and Metabolic Dysfunctions via Production of Succinate and Secondary Bile Acids. *Cell Rep* **26**, 222-235 e225, doi:10.1016/j.celrep.2018.12.028 (2019).
35 Ling, C. *et al.* FAAP100 is essential for activation of the Fanconi anemia-associated DNA damage response pathway. *EMBO J* **26**, 2104-2114, doi:10.1038/sj.emboj.7601666 (2007).
36 Kim, H. S. *et al.* Endonuclease EEPD1 Is a Gatekeeper for Repair of Stressed Replication Forks. *J Biol Chem* **292**, 2795-2804, doi:10.1074/jbc.M116.758235 (2017).
37 Zucker, S. N. *et al.* Nrf2 amplifies oxidative stress via induction of Klf9. *Mol Cell* **53**, 916-928, doi:10.1016/j.molcel.2014.01.033 (2014).
38 Yasuda, S. *et al.* Diacylglycerol kinase eta augments C-Raf activity and B-Raf/C-Raf heterodimerization. *J Biol Chem* **284**, 29559-29570, doi:10.1074/jbc.M109.043604 (2009).
39 Murdoch, H. *et al.* Periplakin interferes with G protein activation by the melanin-concentrating hormone receptor-1 by binding to the proximal segment of the receptor C-terminal tail. *J Biol Chem* **280**, 8208-8220, doi:10.1074/jbc.M405215200 (2005).
40 Gerke, P. *et al.* Neuronal expression and interaction with the synaptic protein CASK suggest a role for Neph1 and Neph2 in synaptogenesis. *J Comp Neurol* **498**, 466-475, doi:10.1002/cne.21064 (2006).
41 Chen, H., Duncan, I. C., Bozorgchami, H. & Lo, S. H. Tensin1 and a previously undocumented family member, tensin2, positively regulate cell migration. *Proc Natl Acad Sci U S A* **99**, 733-738, doi:10.1073/pnas.022518699 (2002).
42 O'Mahony, A. *et al.* NF-kappaB/Rel regulates inhibitory and excitatory neuronal function and synaptic plasticity. *Mol Cell Biol* **26**, 7283-7298, doi:10.1128/MCB.00510-06 (2006).
43 Gerlai, R., Adams, B., Fitch, T., Chaney, S. & Baez, M. Performance deficits of mGluR8 knockout mice in learning tasks: the effects of null mutation and the background genotype. *Neuropharmacology* **43**, 235-249, doi:10.1016/s0028-3908(02)00078-3 (2002).
44 Shao, X. *et al.* HMG-CoA synthase 2 drives brain metabolic reprogramming in cocaine exposure. *Neuropharmacology* **148**, 377-393, doi:10.1016/j.neuropharm.2017.10.001 (2019).
45 Yang, S., Wu, P., Xiao, J. & Jiang, L. Overexpression of COX6B1 protects against I/Rinduced neuronal injury in rat hippocampal neurons. *Mol Med Rep* **19**, 4852-4862, doi:10.3892/mmr.2019.10144 (2019).

46 Ochiai, Y. *et al.* The blood-brain barrier fatty acid transport protein 1 (FATP1/SLC27A1) supplies docosahexaenoic acid to the brain, and insulin facilitates transport. *J Neurochem* **141**, 400-412, doi:10.1111/jnc.13943 (2017).

47 Kautzmann, M. I. *et al.* Membrane-type frizzled-related protein regulates lipidome and transcription for photoreceptor function. *FASEB J* **34**, 912-929, doi:10.1096/fj.201902359R (2020).

48 David, L. A. *et al.* Diet rapidly and reproducibly alters the human gut microbiome. *Nature* **505**, 559-563, doi:10.1038/nature12820 (2014).

49 de La Serre, C. B. *et al.* Propensity to high-fat diet-induced obesity in rats is associated with changes in the gut microbiota and gut inflammation. *Am J Physiol Gastrointest Liver Physiol* **299**, G440-448, doi:10.1152/ajpgi.00098.2010 (2010).

50 Bruce-Keller, A. J. *et al.* Obese-type gut microbiota induce neurobehavioral changes in the absence of obesity. *Biol Psychiatry* **77**, 607-615, doi:10.1016/j.biopsych.2014.07.012 (2015).

51 Leigh, S. J., Kaakoush, N. O., Westbrook, R. F. & Morris, M. J. Minocycline-induced microbiome alterations predict cafeteria diet-induced spatial recognition memory impairments in rats. *Transl Psychiatry* **10**, 92, doi:10.1038/s41398-020-0774-1 (2020).

52 Leigh, S. J., Kaakoush, N. O., Bertoldo, M. J., Westbrook, R. F. & Morris, M. J. Intermittent cafeteria diet identifies fecal microbiome changes as a predictor of spatial recognition memory impairment in female rats. *Transl Psychiatry* **10**, 36, doi:10.1038/s41398-020-0734-9 (2020).

53 Li, J. M. *et al.* Dietary fructose-induced gut dysbiosis promotes mouse hippocampal neuroinflammation: a benefit of short-chain fatty acids. *Microbiome* **7**, 98, doi:10.1186/s40168-019-0713-7 (2019).

54 Kendig, M. D., Westbrook, R. F. & Morris, M. J. Pattern of access to cafeteria-style diet determines fat mass and degree of spatial memory impairments in rats. *Sci Rep* **9**, 13516, doi:10.1038/s41598-019-50113-3 (2019).

55 Takeuchi, T. *et al.* Locus coeruleus and dopaminergic consolidation of everyday memory. *Nature* **537**, 357-362, doi:10.1038/nature19325 (2016).

56 Kempadoo, K. A., Mosharov, E. V., Choi, S. J., Sulzer, D. & Kandel, E. R. Dopamine release from the locus coeruleus to the dorsal hippocampus promotes spatial learning and memory. *Proc Natl Acad Sci U S A* **113**, 14835-14840, doi:10.1073/pnas.1616515114 (2016).

57 Azevedo, E. P. *et al.* A Role of Drd2 Hippocampal Neurons in Context-Dependent Food Intake. *Neuron* **102**, 873-886 e875, doi:10.1016/j.neuron.2019.03.011 (2019).

Figure 1

Figures and Legends

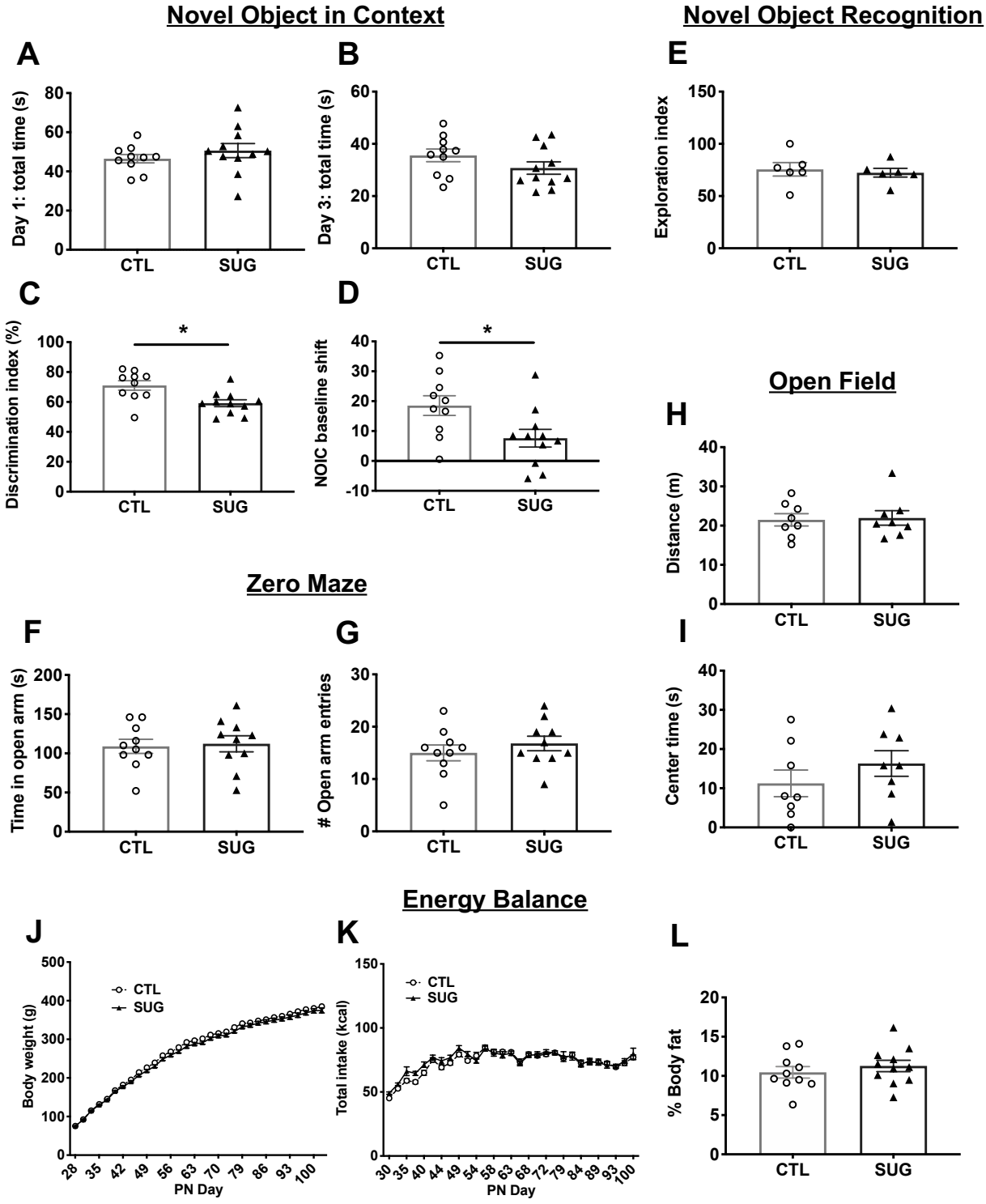

Figure 1: Early-life sugar consumption negatively impacts hippocampal-dependent memory function. (A,B) Early life sugar consumption had no effect on total exploration time in the Novel Object in Context (NOIC) task. (C,D) discrimination index and discrimination shift from baseline were significantly reduced by early life sugar consumption, indicating impaired hippocampal function ($P<.05$, n=10,11; two-tailed, type 2 Student's T-test). (E) There were no differences in exploration index in the Novel Object Recognition (NOR task) (n=6; two-tailed, type 2 Student's T-test). (F, G) There were no differences in time spent in the open arm or the number of entries into the open arm in the Zero Maze task for anxiety-like behavior (n=10,11; two-tailed, type 2 Student's t-test). (H, I) There were no differences in distance travelled or time spent in the center arena in the Open Field task (n=10,11; two-tailed, type 2 Student's T-test). (J-K) Body weights and did not differ between the groups and there was no effect of treatment on total kcal intake while animals had access to early life sugar (n=10,11; two-way repeated measures ANOVA). (L) There were no differences in body composition between rats fed early life sugar and controls (n=10,11; two-tailed, type 2 Student's T-test). CTL=control, SUG= sugar, PN= post-natal day; data shown as mean $\pm$ SEM.

Figure 2

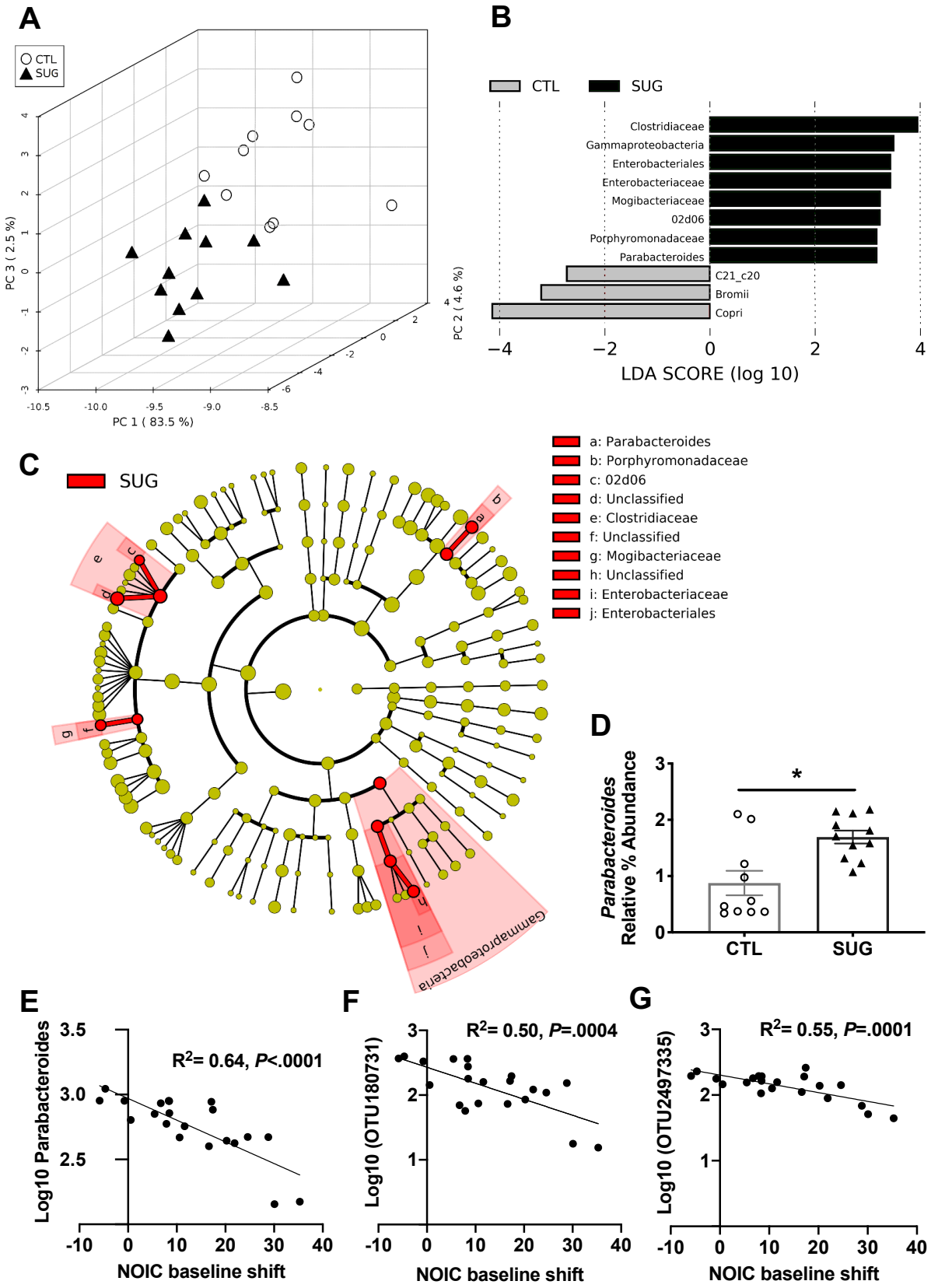

542

Figure 2: Effect of adolescent sugar consumption on the gut microbiome in rats

(A) Principal component analysis showing separation between fecal microbiota of rats fed early life sugar or controls (n=11, 10; dark triangles= sugar, open circles= control). (B) Results from LEfSe analysis showing Linear Discriminate Analysis (LDA) scores for microbiome analysis of fecal samples of rats fed early life sugar or controls. (C) A cladogram representing the results from the LEfSe analysis with class as the outer most taxonomic level and species at the inner most level. Taxa in red are elevated in the sugar group. (D) Relative % abundance of fecal *Parabacteroides* were significantly elevated in rats fed early life sugar ($P<.05$; n=11, 10, two-tailed, type 2 Student's T-test). (E) Linear regression of log normalized fecal *Parabacteroides* counts against shift from baseline performance scores in the novel object in context task (NOIC) across all groups tested (n=21). (E,F) Linear regression of the most abundant fecal *Parabacteroides* OTUs against shift from baseline performance scores in NOIC across all groups tested (n=21). *$P<0.05$; data shown as mean $\pm$ SEM.

Figure 3

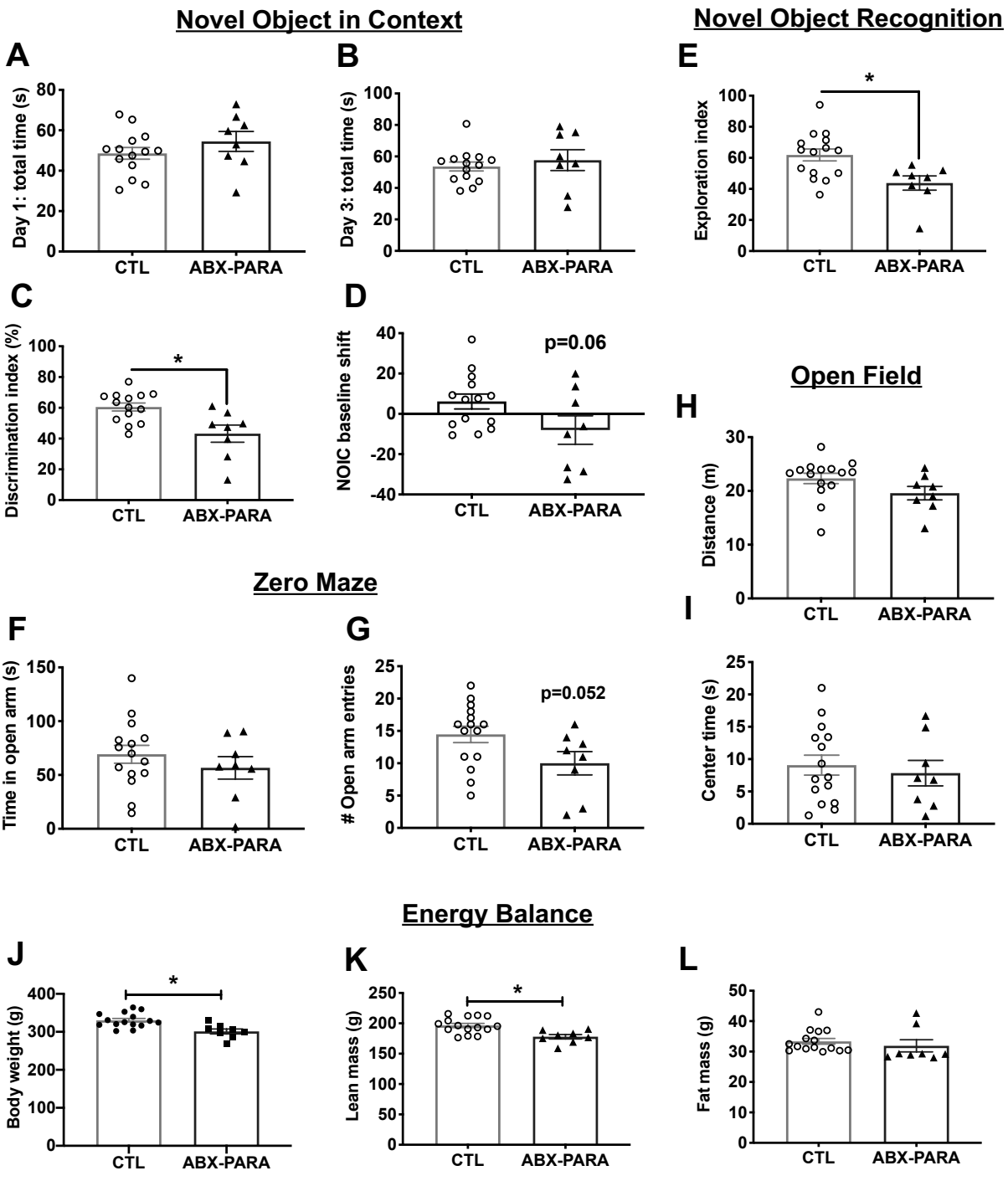

Figure 3: Early-life enrichment with *Parabacteroides* negatively impacts neurocognitive function (A, B) Early-life enrichment with a 1:1 ratio of *P. johnsonii* and *P. distasonis* had no effect on total exploration time in the Novel Object in Context (NOIC) task. (C, D) Discrimination index was significantly reduced and discrimination shift from baseline tended to be reduced by enrichment with *P. johnsonii* and *P. distasonis*, indicating impaired hippocampal function (P<.05, n=14,8; two-tailed, type 2 Student's T-test). (E) There was a significant reduction in the exploration index in the Novel Object Recognition (NOR task), indicating impaired perirhinal cortex function (P<.05, n=14, 8; two-tailed, type 2 Student's T-test). (F, G) There were no differences in time spent in the open arm but there was a trend toward a reduced number of entries into the open arm by animals with *P. johnsonii* and *P. distasonis* enrichment in the Zero Maze task for anxiety-like behavior (P=.052, n=14, 8; two-tailed, type 2 Student's T-test). (H, I) There were no differences in distance travelled or time spent in the center arena in the Open Field task (n=14, 8; two-tailed, type 2 Student's T-test). (J-L) Body weights and lean mass were significantly reduced in animals enriched with *P. johnsonii* and *P. distasonis*, but body fat did not differ between the groups (P<.05, n=14, 8; two-tailed, type 2 Student's T-test). CTL=control, ABX-PARA= *P. johnsonii* and *P. distasonis* enriched, PN= post-natal day; data shown as mean ± SEM.

Figure 4

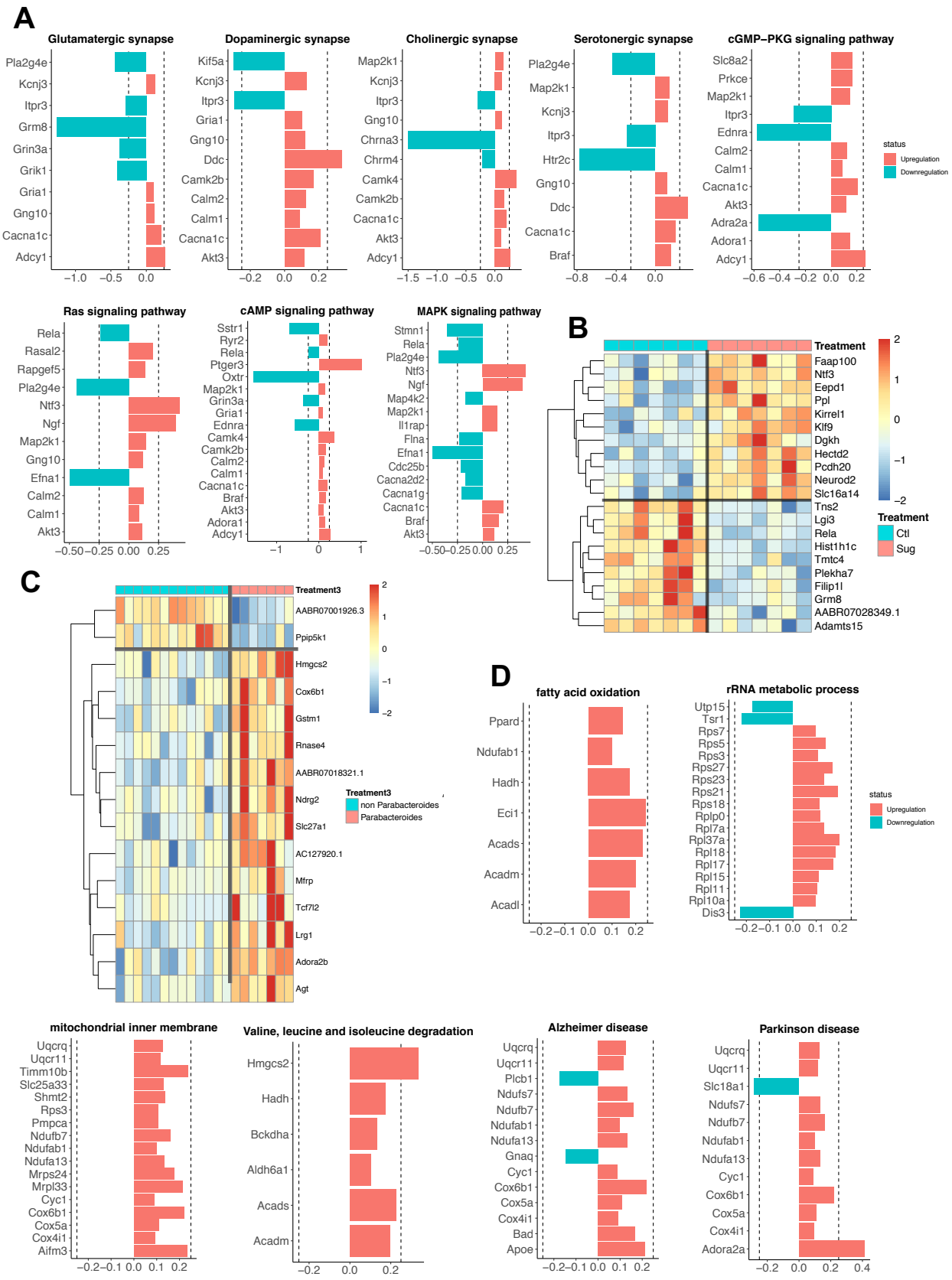

578

Figure 4: Effect of early life sugar or targeted *Parabacteroides* enrichment on hippocampal gene expression (A) Pathway analyses for differentially expressed genes (DEGs) at a p-value < 0.01 in hippocampal tissue punches from rats fed early life sugar compared with controls. Upregulation by sugar is shown in red and downregulation by sugar in blue. (B) A heatmap depicting DEGs that survived the Benjamini-Hochberg corrected FDR of P< 0.05 in rats fed early life sugar compared with controls. Warmer colors (red) signify an increase in gene expression and cool colors (blue) a reduction in gene expression by treatment (CTL=control, SUG= early life sugar; n=7/group). (C) A heatmap depicting DEGs that survived the Benjamini-Hochberg corrected FDR of P< 0.05 in rats with early life *Parabacteroides* enrichment compared with controls. Warmer colors (red) signify an increase in gene expression and cool colors (blue) a reduction in gene expression by treatment (n=7, 14). (D) Pathway analyses for differentially expressed genes (DEGs) at a P-value < 0.01 in rats enriched with *Parabacteroides* compared with controls. Upregulation by *Parabacteroides* transfer is shown in red and downregulation in blue. Dotted line indicates ±0.25 log2 fold change.

Methods and Materials

Experimental Subjects

Juvenile male Sprague Dawley rats (Envigo; arrival post natal day (PN) 26-28; 50-70g) were housed individually in standard conditions with a 12:12 light/dark cycle. All rats had ad libitum access to water and Lab Diet 5001 (PMI Nutrition International, Brentwood, MO; 29.8 % kcal from protein, 13.4% kcal from fat, 56.7% kcal from carbohydrate), with modifications where noted. All experiments were performed in accordance with the approval of the Animal Care and Use Committee at the University of Southern California.

Experiment 1

Twenty one juvenile male rats (PN 26-28) were divided into two groups with equal body weight and given ad libitum access to: 1) 11% weight-by-volume (w/v) solution containing monosaccharide ratio of 65% fructose and 35% glucose in reverse osmosis-filtered water (SUG; n=11) or 2) an extra bottle of reverse osmosis-filtered water (CTL; n=10). This solution was chosen to model commonly consumed sugar-sweetened beverages in humans in terms of both caloric content and monosaccharide ratio[1]. Additionally, all rats were given ad libitum access to water and standard rat chow. Food intake, solution intake and body weights were monitored thrice weekly except where prohibited due to behavioral testing. At PN 60, rats underwent Novel Object in Context (NOIC) testing, to measure hippocampal-dependent episodic contextual memory. At PN 67 rats underwent anxiety testing in the Zero Maze, followed by body composition

testing at PN 70 and an intraperitoneal glucose tolerance test (IP GTT) at PN 84. Fecal and cecal samples were collected prior to sacrifice at PN 104 (for details on all procedures, see supplemental materials).

In a separate cohort of juvenile male rats (n=8/group) animals were treated as above, but on PD day 60 rats were tested in the Novel Object Recognition (NOR) and Open Field (OF) tasks, with two days in between tasks. Animals were sacrificed and tissue punches were collected from the dorsal hippocampus on PN day 65. Tissue punches were flash frozen in isopentane packed in dry ice and stored at -80°C until further analyses.

Experiment 2

Twenty-three juvenile male rats (PN 26-28) were divided into two groups and received a gavage twice daily (12 hours apart) for 7 days (only one treatment was given on day 7) of either (1) saline (SAL; n=8), or (2) a cocktail of antibiotics consisting of Vancomycin (50 mg/kg), Neomycin (100 mg/kg), and Metronidazole (100 mg/kg) along with 1 mg/mL of ampicillin in their drinking water (ABX; n=15), which is a protocol modified from [2]. Animals were housed in fresh, sterile cages on Day 3 of the antibiotic or saline treatment, and again switched to fresh sterile cages on Day 7 after the final gavage. All animals were maintained on sterile, autoclaved water and chow for the remainder of the experiment. Rats in the ABX group were given water instead of ampicillin solution on Day 7. Animals in the ABX group were further subdivided to receive either gavage of a 1:1 ratio of *Parabacteroides distasonis* and *Parabacteroides johnsonii* (PARA; n=8) or saline (SAL; n=7) thirty six hours after the last ABX treatment. To minimize potential

contamination, rats were handled minimally for 14 days. Cage changes occurred once weekly at which time animals and food were weighed. Experimenters wore fresh, sterile PPE and weigh boxes were cleaned with sterilizing solution in between each cage change. On PN 50 rats were tested in NOIC, on PN 60 rats were tested in NOR, on PN 62 rats were tested in the Zero Maze, followed by Open Field on PN 64. On PN 73 rats were given an IP GTT, and on PN 76 body composition was tested. Rats were sacrificed at PN 83 and dorsal hippocampus tissue punches were collected on PN day 65. Tissue punches were flash frozen in isopentane packed in dry ice and stored at -80°C until further analyses.

IP glucose tolerance test (IP GTT)

Animals were food restricted 24 hours prior to IP GTT. Immediately prior to the test, baseline blood glucose readings were obtained from tail tip and recorded by a blood glucose meter (One touch Ultra2, LifeScan Inc., Milpitas, CA). Each animal was then intraperitoneally (IP) injected with dextrose solution (0.923g/ml by body weight) and tail tip blood glucose readings were obtained at 30, 60, 90, and 120 min after IP injections, as previously described [3].

Zero Maze

The Zero Maze is an elevated circular track (63.5 cm fall height, 116.8cm outside diameter), divided into four equal length sections. Two sections were open with 3 cm high curbs, whereas the 2 other closed sections contained 17.5 cm high walls. Animals are placed in the maze facing the open section of the track in a room with ambient lighting for 5 min while the experimenter watches the animal from a monitor outside of

the room. The experimenter records the total time spent in the open sections (defined as the head and front two paws in open arms), and the number of crosses into the open sections from the closed sections.

Novel object in context task (NOIC)

NOIC measures episodic contextual memory based on the capacity for an animal to identify which of two familiar objects it has never seen before in a specific context. Procedures were adapted from prior reports [4, 5]. Briefly, rats are habituated to two distinct contexts on subsequent days (with the habituation order counterbalanced by group) for 5-min sessions: Context 1 is a semi-transparent box (15in W x 24in L x 12in H) with orange stripes and Context 2 is a grey opaque box (17in W x 17in L x 16in H) (Context identify assignments counterbalanced by group). Day 1 of NOIC begins with each animal being placed in Context 1 containing two distinct objects placed in opposite corners: a 500ml jar filled with blue water (Object A) and a square glass container (Object B) (Object assignments counterbalanced by group). On day 2 of NOIC, animals are placed in Context 2 with duplicates of one of the objects. On NOIC day 3, rats are placed in Context 2 with Objects A and Object B. One of these objects is not novel to the rat, but its placement in Context 2 is novel. All sessions are 5 minutes long and are video recorded. The time spent investigating each object is recorded from the video recordings by an experimenter who is blinded to the treatment groups. Exploration is defined as sniffing or touching the object with the nose or forepaws. The task is scored by calculating the time spent exploring the Novel Object to the context divided by the time spent exploring both Objects A and B combined, which is the novelty or “discrimination index”. Rats with an intact hippocampus will preferentially investigate the object that is

97 novel to Context 2, given that this object is a familiar object yet is now presented in a
98 novel context, whereas hippocampal inactivation impairs the preferential investigation
99 of the object novel to Context 2 [4].
100
101 Novel Object Recognition
102 The apparatus used for NOR is a grey opaque box (17in W x 17in L x 16in H). Procedures
103 are adapted from [6]. Rats are habituated to the empty arena and conditions for 10
104 minutes on the day prior to testing. The test begins with a 5 minute familiarization
105 phase, where rats are placed in the center of the arena with two identical copies of the
106 same object to explore. The objects were either two identical cans or two identical
107 bottles, counterbalanced by treatment group. Animals are then removed from the arena
108 and placed in the home cage for 5 minutes. The arena and objects are cleaned with 10%
109 ethanol solution, and one of the objects in the arena is replaced with a different one
110 (either the can or bottle, whichever the animal has not previously seen, i.e., the "novel
111 object"). Animals are again placed in the center of the arena and allowed to explore for 3
112 minutes. Time spent exploring the objects is recorded via video recording and analyzed
113 using Any-maze activity tracking software (Stoelting Co., Wood Dale, IL).
114
115 Open Field
116 Open field measures general activity level and also anxiety in the rat. A large gray bin,
117 60 cm (L) X 56 CM (W) is placed under diffuse even lighting (30 lux). A center zone is
118 identified and marked in the bin (19 cm L X 17.5 cm W). A video camera is placed
119 directly overhead and animals are tracked using AnyMaze Software (Stoelting Co.,
120 Wood Dale, IL). Animals are placed in the center of the box facing the back wall and

allowed to explore the arena for 10 min while the experimenter watches from a monitor in an adjacent room. The apparatus is cleaned with 10% ethanol after each rat is tested.

Body Composition

Body composition (body fat, lean mass) was measured using LF90 time domain nuclear magnetic resonance (Bruker NMR minispec LF 90II, Bruker Daltonics, Inc.).

Bacterial transfer

Parabacteroides distasonis (ATCC 8503) was cultured under anaerobic conditions at 37C in Reinforced Clostridial Medium (RCM, BD Biosciences). *Parabacteroides johnsonii* (DSM 18315) was grown in anaerobic conditions in PYG medium (modified, DSM medium 104). Cultures were authenticated by full-length 16S rRNA gene sequencing. For bacterial enrichment, 10^9 colony-forming units of both *P. distasonis* and *P. johnsonii* were suspended in 500 uL pre-reduced PBS and orally gavaged into antibiotic-treated rats. When co-administered, a ratio of 1:1 was used for *P. distasonis* and *P. johnsonii*.

Gut microbiota DNA extraction and 16s rRNA gene sequencing

All samples were extracted and sequenced according to the guidelines and procedures established by the Earth Microbiome Project [7]. DNA was extracted from fecal and cecal samples using the MO BIO PowerSoil DNA extraction kit. PCR targeting the V4 region of the 16S rRNA bacterial gene was performed with the 515F/806R primers, utilizing the protocol described in Caporaso et al.[8]. Amplicons were barcoded and pooled in equal concentrations for sequencing. The amplicon pool was purified with the MO BIO

UltraClean PCR Clean-up kit and sequenced by the 2 x 150bp MiSeq platform at the Institute for Genomic Medicine at UCSD. All sequences were deposited in Qiita Study 11255 as raw FASTQ files. Sequences were demultiplexed using Qiime-1 based "split libraries" with the forward reads only dropping. Demultiplexed sequences were then trimmed evenly to 100 bp and 150 bp to enable comparison to other studies for metaanalysis. Trimmed sequences were matched to known OTUs at 97% identity.

Hippocampal RNA extraction and sequencing

Hippocampi from rats treated with or without sugar or *Parabacteroides* were subject to RNA-seq analysis. Total RNA was extracted according to manufacturer's instructions using RNeasy Lipid Tissue Mini Kit (Qiagen, Hilden, Germany). Total RNA was checked for degradation in a Bioanalyzer 2100 (Agilent, Santa Clara, CA, USA). Quality was very high for all samples, and libraries were prepared from 1 ug of total RNA using a NuGen Universal Plus mRNA-seq Library Prep Kit (Tecan Genomics Inc. Redwood City, CA). Final library products were quantified using the Qubit 2.0 Fluorometer (Thermo Fisher Scientific Inc., Waltham, MA, USA), and the fragment size distribution was determined with the Bioanalyzer 2100. The libraries were then pooled equimolarly, and the final pool was quantified via qPCR using the Kapa Biosystems Library Quantification Kit, according to manufacturer's instructions. The pool was sequenced in an Illumina NextSeq 550 platform (Illumina, San Diego, CA, USA), in Single-Read 75 cycles format, obtaining about 25 million reads per sample. The preparation of the libraries and the sequencing was performed at the USC Genome Core (http://uscgenomecore.usc.edu/)

RNA-seq quality control

Data quality checks were performed using the FastQC tool (http://www.bioinformatics.babraham.ac.uk/projects/fastqc) and low quality reads were trimmed with Trim_Galore (http://www.bioinformatics.babraham.ac.uk/projects/trim_galore/). RNA-seq reads passing quality control were mapped to *Rattus novegicus* transcriptome (Rnor6) and quantified with Salmon [9]. Salmon directly mapped RNA-seq reads to Rat transcriptome and quantified transcript counts. Txiimport [10] were used to convert transcript counts into gene counts. Potential sample outliers were detected by principle component analysis (PCA) and one control and one treatment sample from the *Parabacteroides* experiment were deemed outliers (Supplementary Figure 6A, B) and removed.

Identification of differentially expressed genes (DEGs)

DESeq2[11] were used to conduct differential gene expression analysis between sugar treatment and the corresponding controls, or between *Parabacteroides* treatment and the corresponding controls. Low-abundance genes were filtered out and only those having a mean raw count > 1 in more than 50% of the samples were included. Differentially expressed genes were detected by DESeq2 with default settings. Significant DEGs were defined as Benjamini-Hochberg (BH) adjusted false discovery rate (FDR) < 0.05. For heatmap visualization, genes were normalized with variance stabilization transformation implemented in DESeq2, followed by calculating a z-score for each gene.

Pathway analyses of DEGs

For the pathway analyses, DEGs at p-value < 0.01 was used. Pathway enrichment analysis were conducted using enrichr[12] by intersecting each signature with pathways or gene sets from KEGG[13], gene ontology biological pathways (GOBP), Cellular Component (GOCP), Molecular Function (GOMF)[14] and Wikipathways[15]. Pathways at FDR < 0.05 were considered significant. Unless otherwise specified, R 3.5.2 was used for the analysis mentioned in the RNA sequencing section.

Additional Statistical methods

Data are presented as means ± SEM. For analytic comparisons of body weight, total food intake, and chow intake, groups were compared using repeated measures ANOVA in Prism software (GraphPad Inc., version 8.0). When significant differences were detected, Sidak post-hoc test for multiple comparisons was used. Area under the curve (AUC) for the IP GTT testing was also calculated using Prism. All other statistical analyses were performed using Student's two-tailed unpaired t tests in excel software (Microsoft Inc., version 15.26). For all analyses, statistical significance was set at $P<0.05$.

1. Walker RW, Dumke KA, Goran MI. Fructose content in popular beverages made with and without high-fructose corn syrup. *Nutrition* **30**, 928-935 (2014).

2. Olson CA, Vuong HE, Yano JM, Liang QY, Nusbaum DJ, Hsiao EY. The Gut Microbiota Mediates the Anti-Seizure Effects of the Ketogenic Diet. *Cell* **173**, 1728-1741 e1713 (2018).

3. Hsu TM*, et al.* Effects of sucrose and high fructose corn syrup consumption on spatial memory function and hippocampal neuroinflammation in adolescent rats. *Hippocampus* **25**, 227-239 (2015).

4. Martinez MC, Villar ME, Ballarini F, Viola H. Retroactive interference of object-in-context long-term memory: role of dorsal hippocampus and medial prefrontal cortex. *Hippocampus* **24**, 1482-1492 (2014).

5. Balderas I, Rodriguez-Ortiz CJ, Salgado-Tonda P, Chavez-Hurtado J, McGaugh JL, Bermudez-Rattoni F. The consolidation of object and context recognition memory involve different regions of the temporal lobe. *Learn Mem* **15**, 618-624 (2008).

6. Beilharz JE, Maniam J, Morris MJ. Short exposure to a diet rich in both fat and sugar or sugar alone impairs place, but not object recognition memory in rats. *Brain Behav Immun* **37**, 134-141 (2014).

7. Thompson LR*, et al.* A communal catalogue reveals Earth's multiscale microbial diversity. *Nature* **551**, 457-463 (2017).

8. Caporaso JG*, et al.* Ultra-high-throughput microbial community analysis on the Illumina HiSeq and MiSeq platforms. *ISME J* **6**, 1621-1624 (2012).

9. Patro R, Duggal G, Love MI, Irizarry RA, Kingsford C. Salmon provides fast and bias-aware quantification of transcript expression. *Nat Methods* **14**, 417-419 (2017).

10. Soneson C, Love MI, Robinson MD. Differential analyses for RNA-seq: transcript-level estimates improve gene-level inferences. *F1000Res* **4**, 1521 (2015).

11. Anders S, Huber W. Differential expression analysis for sequence count data. *Genome Biol* **11**, R106 (2010).

12. Kuleshov MV*, et al.* Enrichr: a comprehensive gene set enrichment analysis web server 2016 update. *Nucleic Acids Res* **44**, W90-97 (2016).

13. Kanehisa M, Furumichi M, Tanabe M, Sato Y, Morishima K. KEGG: new perspectives on genomes, pathways, diseases and drugs. *Nucleic Acids Res* **45**, D353-D361 (2017).

14. The Gene Ontology C. Expansion of the Gene Ontology knowledgebase and resources. *Nucleic Acids Res* **45**, D331-D338 (2017).

15. Slenter DN*, et al.* WikiPathways: a multifaceted pathway database bridging metabolomics to other omics research. *Nucleic Acids Res* **46**, D661-D667 (2018).

Extended Data

Extended Data Fig. 1

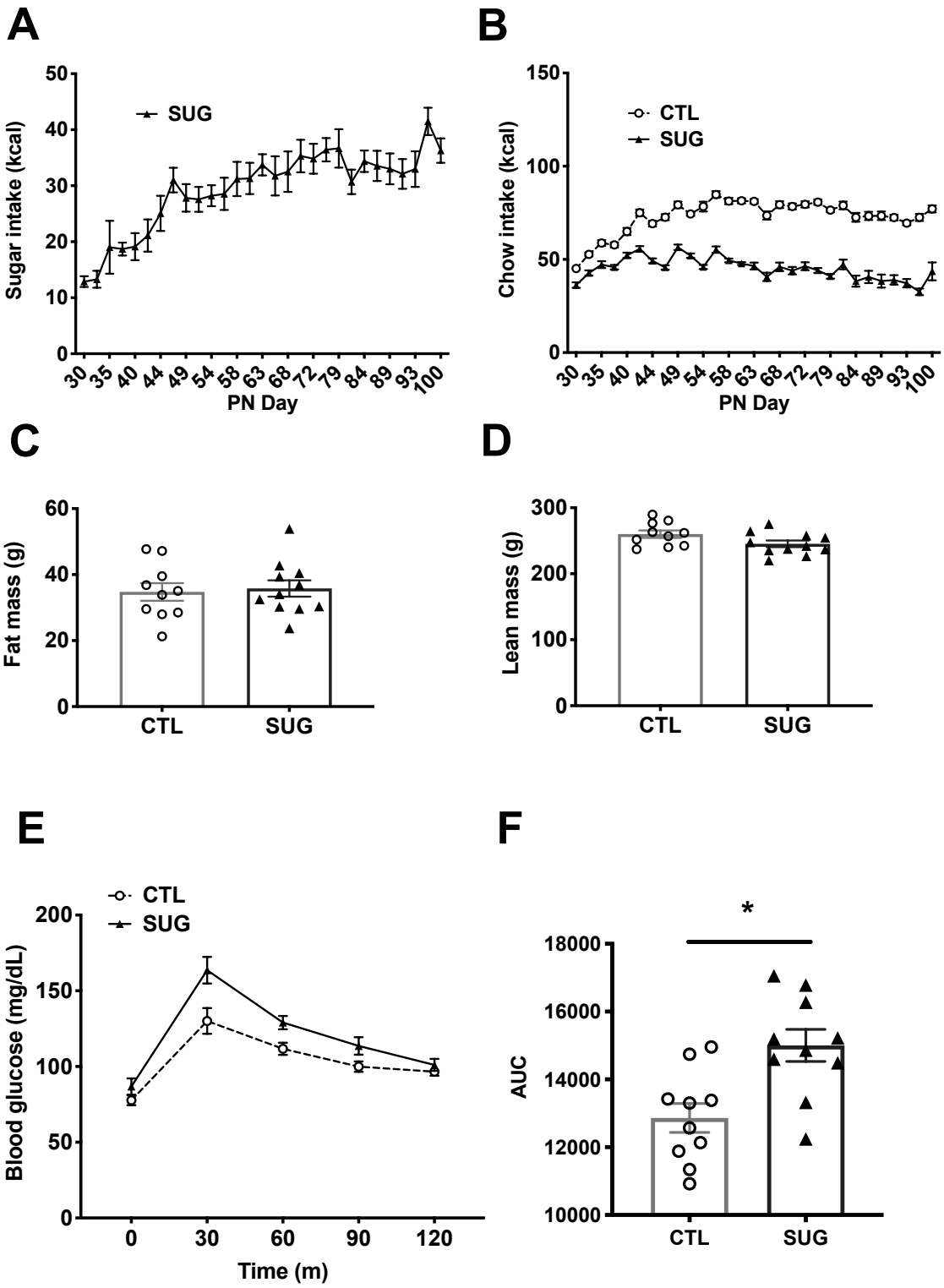

Extended Data Fig. 1 Effect of early life sugar consumption on food intake and metabolic measures (A) kcals from sugar over the feeding period beginning at post-natal day (PN) 28 with the first measurement taken on PN 30 (n=11). (B) Kcals from chow intake were lower throughout the feeding period in animals fed early life sugar (n=10,11). (C, D) there were no differences in fat mass or lean mass (n=10,11; two-tailed, type 2 Student's T-test). (E, F) Results from the intraperitoneal glucose tolerance test show an elevated area under the curve (AUC) in rodents fed sugar solutions during early life (n=10,11; two-tailed, type 2 Student's T-test; $P<.05$). CTL=control, SUG= sugar, PN= post-natal day; data shown as mean $\pm$ SEM.

Extended Data Fig. 2

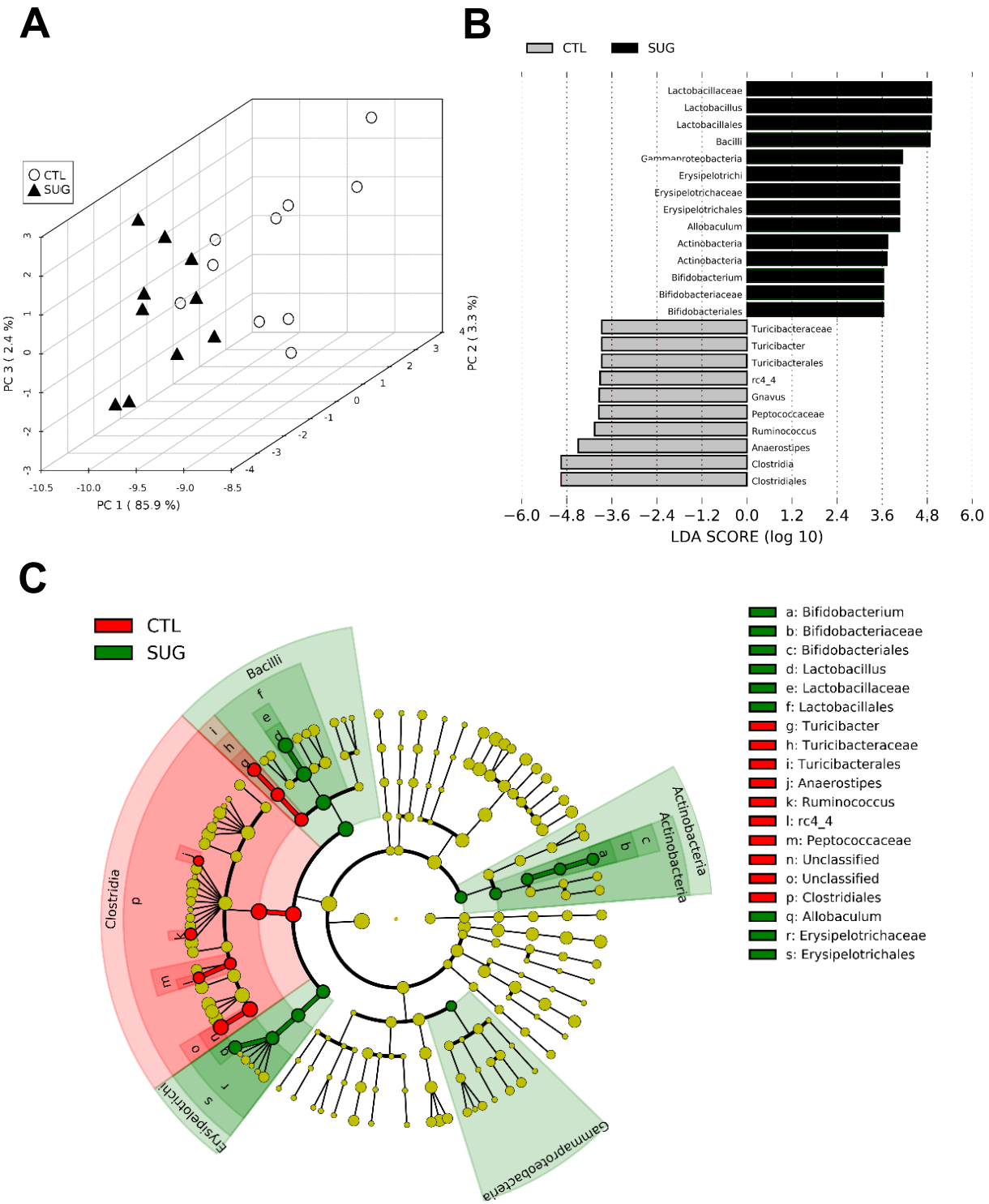

Extended Data Fig. 2 Effect of early life sugar consumption on the rat cecal microbiota (A) Principal component analysis (PCA) was run using all phylogenic levels (112 normalized taxa abundances) and shows different clustering patterns based on overall cecal microbial profiles. (B) Linear discriminant analysis (LDA) Effect Size (LEfSe), run using the GALAXY platform, identified characteristic features of the cecal microbiota of rats fed a control diet or early life sugar. Relative differences among groups were used to rank the features with the LDA score set at 2. (C) Identified taxa are displayed by scores and on a phylogenic cladogram. CTL=control, SUG= sugar.

Extended Data Fig. 3

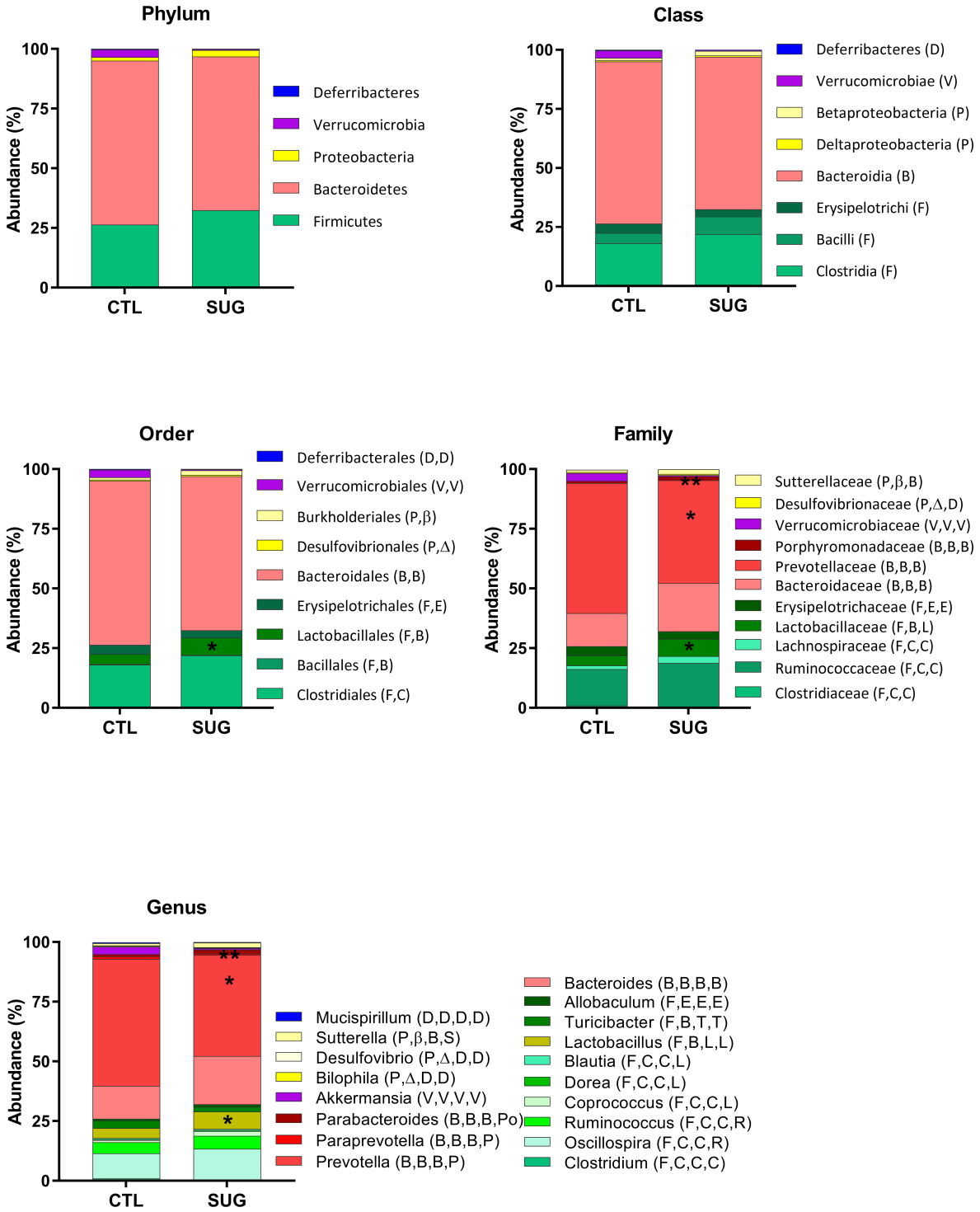

Extended Data Fig. 3 Effect of early life sugar consumption on the rat fecal microbiota. Filtered bacterial abundances by taxonomic levels phylum, class, order, family, genus in fecal samples from rats fed a control diets or early life sugar. Differences in abundances were assessed by Mann-Whitney non-parametric test. * $p<0.05$, *** $p<0.001$. CTL=control, SUG= sugar.

Extended Data Fig. 4

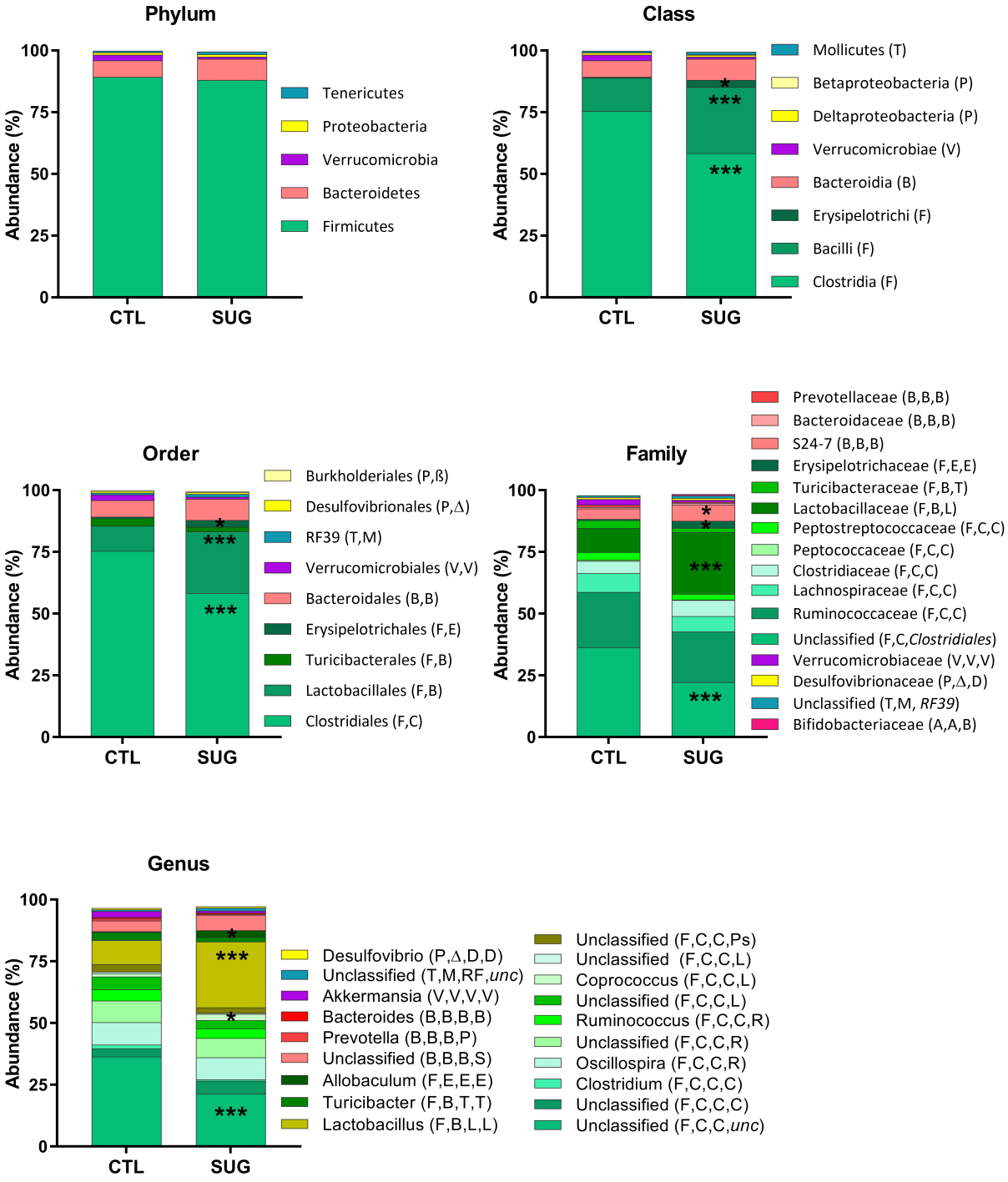

Extended Data Fig. 4 Effect of early life sugar consumption on the rat cecal microbiota: Filtered bacterial abundances by taxonomic levels phylum, class, order, family, genus in cecal samples from rats fed a control diets or early life sugar. Differences in abundances were assessed by Mann-Whitney non-parametric test. * p<0.05, *** p<0.001. CTL=control, SUG= sugar.

Phylogenic taxonomy legend:

Phylum		Class		Order		Family		Genus
F	*Firmicutes*	C	*Clostridia*	C	*Clostridiales*	C	*Clostridiaceae*	*Clostridium*
						L	*Lachnospiraceae*	*Coprococcus*
								Blautia
								Dorea
						P	*Peptococcaceae*	
						Ps	*Peptostreptococcaceae*	
						R	*Ruminococcaceae*	*Oscillospira*
								Ruminococcus
		B	*Bacilli*	L	*Lactobacillales*	L	*Lactobacillaceae*	*Lactobacillus*
				T	*Turicibacterales*	T	*Turicibacteraceae*	*Turicibacter*
				B	*Bacillales*			
		E	*Erysipelotrichi*	E	*Erysipelotrichales*	E	*Erysipelotrichaceae*	*Allobaculum*
B	*Bacteroidetes*	B	*Bacteroidia*	B	*Bacteroidales*	S	*S24-7*	
						B	*Bacteroidaceae*	*Bacteroides*
						P	*Prevotellaceae*	*Prevotella*
								Paraprevotella
						Po	*Porphyromonadaceae*	*Parabacteroides*
V	*Verrucomicrobia*	V	*Verrucomicrobiae*	V	*Verrucomicrobiales*	V	*Verrucomicrobiaceae*	*Akkermansia*
P	*Proteobacteria*	β	*Betaproteobacteria*	B	*Burkholderiales*	S	*Sutterellaceae*	*Sutterella*
		Δ	*Deltaproteobacteria*	D	*Desulfovibrionales*	D	*Desulfovibrionaceae*	*Desulfovibrio*
								Bilophila
T	*Tenericutes*	M	*Mollicutes*	RF	*RF39*			
D	*Deferribacteres*	D	*Deferribacteres*	D	*Deferribacterales*	D	*Deferribacteraceae*	*Mucispirillum*
A	*Actinobacteria*	A	*Actinobacteria*	B	*Bifidobacter*	B	*Bifidobacteriaceae*	

Extended Data Fig. 5

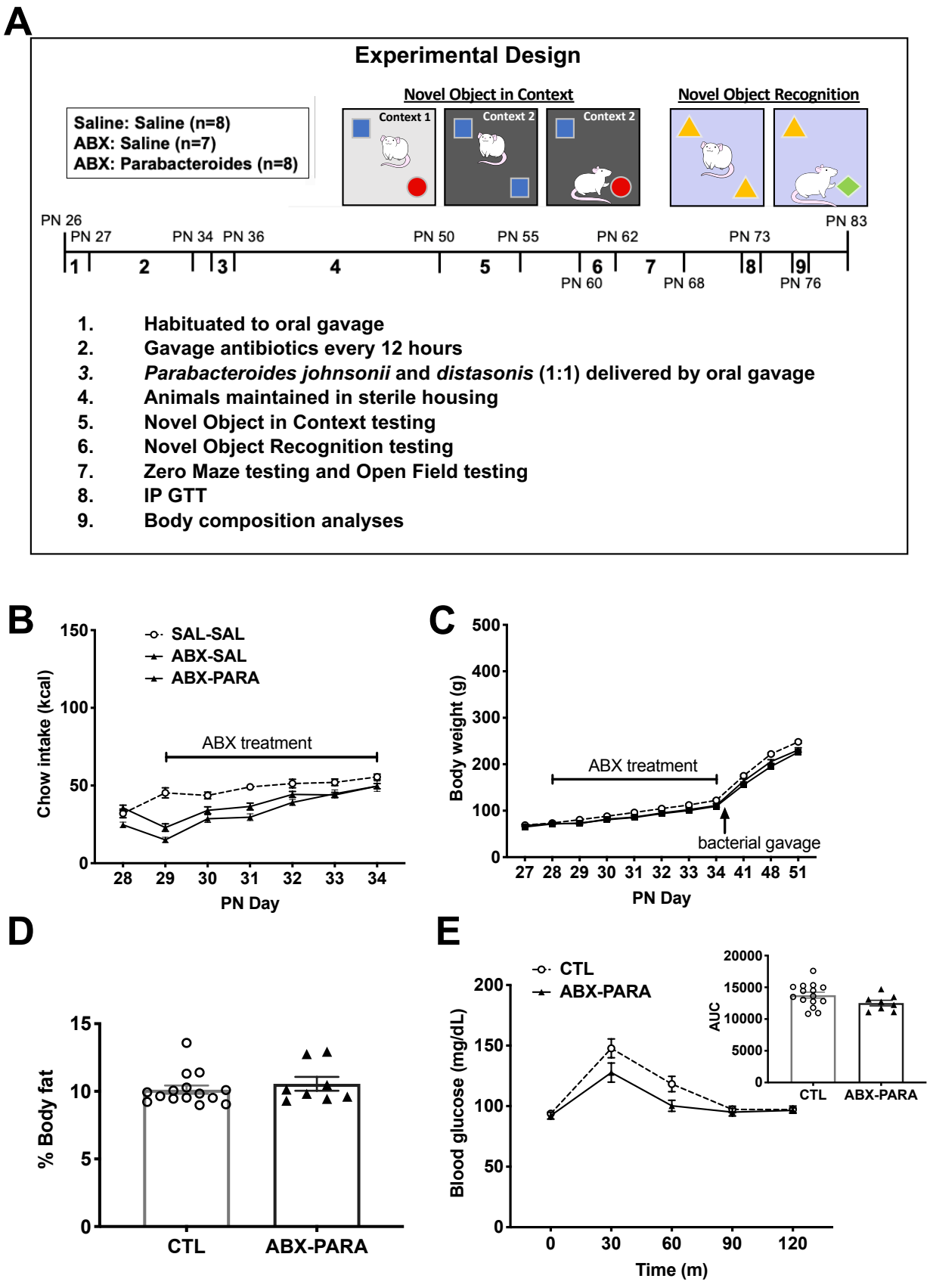

Extended Data Fig. 5. Experimental design, food intake, and metabolic measures for gut *Parabacteroides* enrichment (A) Schematic showing the timeline for the experimental design of the *Parabacteroides* transfer experiment. (B) Effect of antibiotic treatment on food intake (C) and body weight. (D) Effect of gut *Parabacteroides* enrichment on body composition 30 days post treatment (n=15, 8, n.s.). (E) Effect of gut *Parabacteroides* enrichment blood glucose levels during an interaperitoneal glucose tolerance test (IP GTT) (n=15, 8, n.s.) CTL=control, ABX-PARA= *Parabacteroides* enriched, PN= post-natal day; data shown as mean ± SEM.

Extended Data Fig. 6

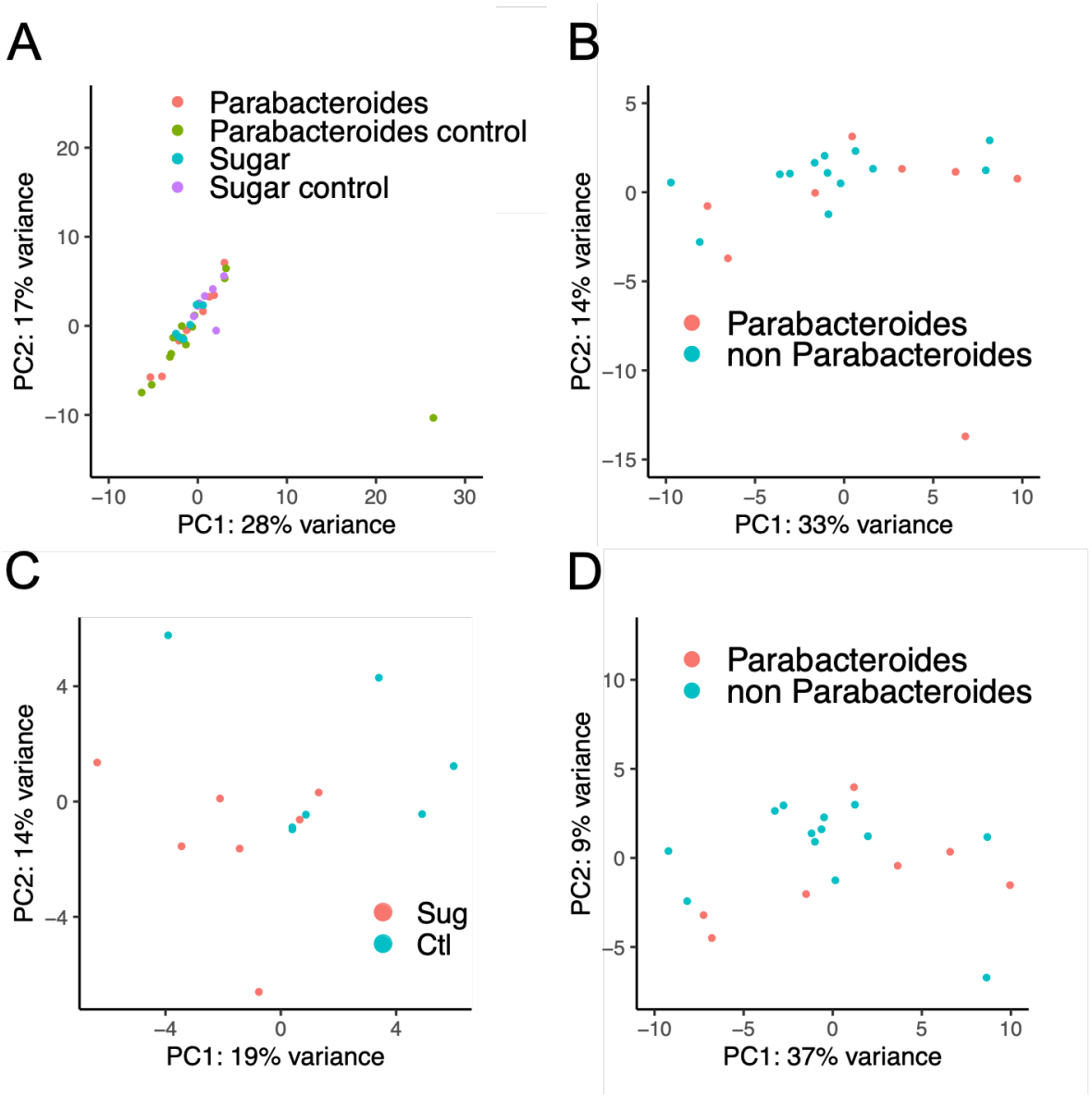

Extended Data Fig. 6. Principal component analyses (PCA) of hippocampal gene expression data to identify outliers (A) PCA identified one control sample (red arrow) as an outlier when all samples from both sugar and *Parabacteroides* enrichment experiments were considered. (B) PCA identified one treatment sample (red arrow) from the *Parabacteroides* experiment as an outlier. After removing the outliers, PCA for the remaining samples from the sugar treatment experiment (C) and those from the *Parabacteroides* enrichment experiments (D).

Extended Data Fig. 7

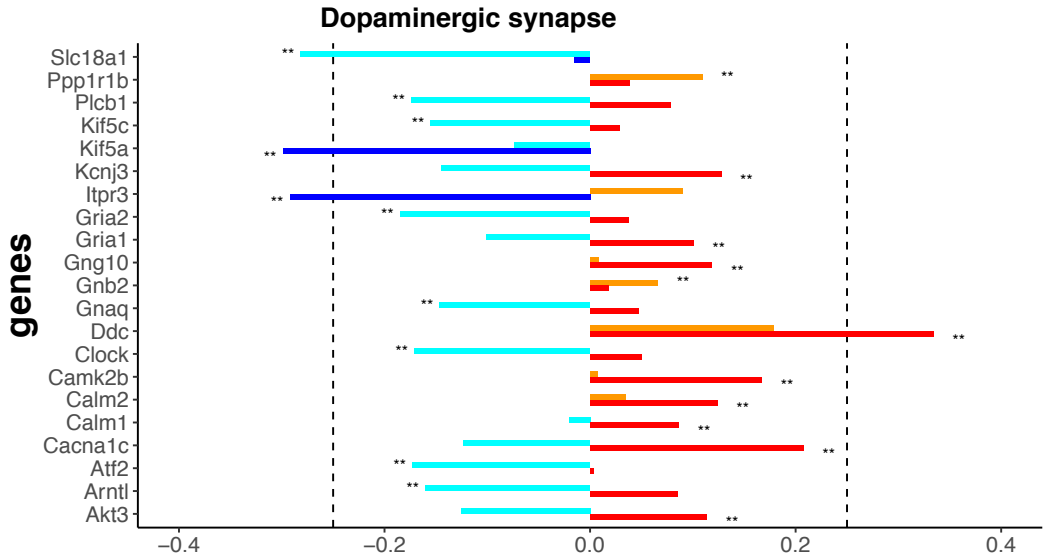

Extended Data Fig 7. Comparison of hippocampal gene expression pathways altered by sugar and *Parabacteriodes* The dopaminergic synapse pathway overlaps in the sugar and *Parabacteroides* transfer experiments. Red= upregulated by sugar, dark blue= downregulated by sugar, orange= upregulated by *Parabacteroides*, light blue= downregulated by *Parabacteroides*. * $P < 0.05$ and ** $P < 0.01$. Dotted line indicated ± 0.25 log2 fold change.

Table 1

Term	Overlap	P.value	Adjusted.P.value	Odds.Ratio	Combined.Score
cAMP signaling pathway	18/211	9.08710002926925e-07	0.000275339130886858	3.922209511	54.56279715
Long-term potentiation	10/67	1.75113958513324e-06	0.000265297647147685	6.862240522	90.96067106
Vascular smooth muscle contraction	14/140	2.31824837751272e-06	0.000234143086128785	4.597701149	59.65378698
Oxytocin signaling pathway	14/154	7.11610557675168e-06	0.000539044997438939	4.179728318	49.54294651
Circadian entrainment	11/99	1.02664310479357e-05	0.000622145721504906	5.108556833	58.68010783
Amphetamine addiction	9/68	1.58699502114579e-05	0.000801432485678624	6.085192698	67.24797055
Calcium signaling pathway	15/189	1.74937542122293e-05	0.000757229646615067	3.648969166	39.96959184
Cholinergic synapse	11/113	3.60773936379843e-05	0.00136643128403866	4.475638287	45.78508194
Axon guidance	14/180	4.14870567165781e-05	0.00139673090945813	3.575989783	36.08219845
Apelin signaling pathway	12/138	4.9577399145753e-05	0.00150219519411632	3.998001	39.62808792
Neurotrophin signaling pathway	11/121	6.78430713999647e-05	0.00186876823947175	4.179728318	40.11834187
Dopaminergic synapse	11/135	0.000181335935857366	0.00457873238039848	3.746275011	32.2747558
Glutamatergic synapse	10/114	0.000194050732212181	0.00452287475848392	4.033071184	34.47223604
Aldosterone synthesis and secretion	9/102	0.0003852671882922	0.00833828271803832	4.056795132	31.89279298
cGMP-PKG signaling pathway	12/172	0.000397324053301256	0.00802594587668537	3.207698476	25.11871164
Inflammatory mediator regulation of TRP channels	10/127	0.000464586599843255	0.00879810873453165	3.620237126	27.78301233
MAPK signaling pathway	16/294	0.000759189930175949	0.0135314440496066	2.502150285	17.97359249
GnRH signaling pathway	8/90	0.000767481845084928	0.0129192777255963	4.086845466	29.31247298
Glioma	7/75	0.0012196493427778	0.0194501974137724	4.291187739	28.79040196
Renin secretion	7/76	0.00131872717084366	0.0199787166382814	4.234724743	28.08083358
Retrograde endocannabinoid signaling	10/150	0.00167349865616307	0.0241461948960672	3.0651341	19.59490832
Neuroactive ligand-receptor interaction	17/348	0.00171069778931894	0.0235609740983472	2.246003435	14.30895981
Serotonergic synapse	9/132	0.00241588944480672	0.0318267174685407	3.134796238	18.88930332
Fc gamma R-mediated phagocytosis	7/87	0.00287625632706458	0.0363127361291903	3.699299775	21.64558595
Regulation of actin cytoskeleton	12/217	0.00294032709499641	0.0356367643913564	2.542507548	14.82087258
Dilated cardiomyopathy (DCM)	7/90	0.00347972133870684	0.0405521371395451	3.575989783	20.24297392
Apoptosis	9/141	0.00375836444668354	0.0421772010127819	2.934702861	16.38670992
Cocaine addiction	5/48	0.00377562901206963	0.040857699666325	4.789272031	26.7202504
Morphine addiction	7/92	0.00393256649864465	0.0410885396237699	3.498250875	19.37493308
Arrhythmogenic right ventricular cardiomyopathy (ARVC)	6/72	0.00476843186679707	0.0481611618546504	3.831417625	20.48175394
Proteoglycans in cancer	11/203	0.00502723467090038	0.0491371646865424	2.491365155	13.18650979
Ras signaling pathway	12/233	0.00518599384881057	0.0491048792559251	2.367914755	12.45947913
response to calcium ion (GO:0051592)	11/80	1.2352727119088e-06	0.00630359664887059	6.32183908	86.00368202
axon guidance (GO:0007411)	15/159	2.11788224048725e-06	0.00540377653660322	4.337453915	56.66924273
nervous system development (GO:0007399)	25/456	2.46003232910435e-05	0.0418451499180649	2.52066949	26.75123758
semaphorin-plexin signaling pathway (GO:0071526)	6/30	3.8991177233796e-05	0.0497429943560153	9.195402299	93.35333482
regulation of cAMP biosynthetic process (GO:0030817)	5/19	4.29910702140572e-05	0.0438766862604667	12.09921355	121.651762
integral component of plasma membrane (GO:0005887)	61/1464	7.0402625056926e-07	0.00031399570775389	1.915708812	27.13879347
dendrite (GO:0030425)	16/216	2.18212117029006e-05	0.00486613020974683	3.405704555	36.55216023
Hypothetical Network for Drug Addiction WP1246	6/31	4.74677094198248e-05	0.00835431685788917	8.898776418	88.59142051

Table 2

	Term	Overlap	P.value	Adjusted.P.v	Old.P.value	Old.Adjusted	Odds.Ratio	Combined.Sc	Genes	database
1	Ribosome	16/170	2.2535714016	0.0006828321	0	0	4.06555711	52.8644159	RPS7;RPS5;F	KEGG_2019_Mouse
2	Alzheimer disease	14/175	5.9653102426	0.0090374450	0	0	3.45572354	33.6136999	NDUFA13;ND	KEGG_2019_Mouse
3	Parkinson disease	12/144	0.0001349676	0.0136317326	0	0	3.59971202	32.0751456	NDUFA13;ND	KEGG_2019_Mouse
4	Valine, leucine and isoleucine degradation	7/56	0.0002964533	0.0224563378	0	0	5.39956803	43.8640434	BCKDHA;ALD	KEGG_2019_Mouse
5	Cardiac muscle contraction	8/78	0.0004410118	0.0267253189	0	0	4.4304148	34.2313287	UQCRQ;COX	KEGG_2019_Mouse
6	Hepatocellular carcinoma	12/171	0.0006547942	0.0330671074	0	0	3.03133644	22.2233021	TCF7L2;SMA	KEGG_2019_Mouse
7	cGMP-PKG signaling pathway	12/172	0.0006895098	0.0298459255	0	0	3.01371239	21.9384086	ATF2;PPP1R	KEGG_2019_Mouse
8	Colorectal cancer	8/88	0.0009893071	0.0374700074	0	0	3.92695857	27.1686854	TCF7L2;SMA	KEGG_2019_Mouse
9	Fatty acid degradation	6/50	0.0009995403	0.0336511912	0	0	5.18358531	35.8093221	ACADL;ECI1;	KEGG_2019_Mouse
10	Thermogenesis	14/231	0.0010310146	0.0312397432	0	0	2.61797238	18.0043508	ATF2;NDUFA	KEGG_2019_Mouse
11	Oxidative phosphorylation	10/134	0.0011365669	0.0313072522	0	0	3.22362271	21.8553336	NDUFA13;ND	KEGG_2019_Mouse
12	Dopaminergic synapse	10/135	0.0012027348	0.0303690537	0	0	3.19974402	21.5123824	ATF2;GRIA2;I	KEGG_2019_Mouse
13	Vascular smooth muscle contraction	10/140	0.0015824106	0.0368823395	0	0	3.08546745	19.8975807	PPP1R12A;AI	KEGG_2019_Mouse
14	Endocrine and other factor-regulated calcium reabsorption	6/55	0.0016548484	0.0358156477	0	0	4.71235028	30.1781074	GNAQ;BDKRI	KEGG_2019_Mouse
15	Pathways in cancer	24/535	0.0016621713	0.0335758610	0	0	1.9377889	12.401133	RET;TCF7L2;	KEGG_2019_Mouse
16	Huntington disease	12/192	0.0017815419	0.0337379513	0	0	2.69978402	17.090378	NDUFA13;ND	KEGG_2019_Mouse
17	Endometrial cancer	6/58	0.0021800554	0.0388562817	0	0	4.46860803	27.3854397	TCF7L2;APC;	KEGG_2019_Mouse
18	Gastric cancer	10/150	0.0026327375	0.0443177484	0	0	2.87976962	17.1050571	TCF7L2;SMA	KEGG_2019_Mouse
19	Non-alcoholic fatty liver disease (NAFLD)	10/151	0.0027627966	0.0440593356	0	0	2.8606983	16.8538379	NDUFA13;ND	KEGG_2019_Mouse
20	SRP-dependent cotranslational protein targeting to membrane (GO:0	16/90	2.3456175755	1.1969686487	0	0	7.67938565	170.277339	RPS7;RPS5;F	GO_Biological_Process_2018
21	protein targeting to ER (GO:0045047)	16/98	8.7398242692	2.2299661623	0	0	7.05249702	147.100707	RPS7;RPS5;F	GO_Biological_Process_2018
22	viral transcription (GO:0019083)	17/114	1.1115537635	1.8907529518	0	0	6.44158994	132.809526	RANBP2;RPS	GO_Biological_Process_2018
23	cotranslational protein targeting to membrane (GO:0006613)	15/94	4.0895658105	5.2172635828	0	0	6.89306558	133.138369	RPS7;RPS5;F	GO_Biological_Process_2018
24	viral gene expression (GO:0019080)	16/111	5.7091825356	5.8267916958	0	0	6.2265289	118.186928	RANBP2;RPS	GO_Biological_Process_2018
25	nuclear-transcribed mRNA catabolic process, nonsense-mediated de	15/113	5.3284114672	4.5318139528	0	0	5.73405455	96.0318102	RPS7;RPS5;F	GO_Biological_Process_2018
26	cellular protein metabolic process (GO:0044267)	31/485	3.8477509014	0.0002805010	0	0	2.76101623	40.7818853	RPLP0;RPL1	GO_Biological_Process_2018
27	cytoplasmic translation (GO:0002181)	10/55	4.6181807744	0.0002945822	0	0	7.85391714	114.573688	RPS7;RPLP0	GO_Biological_Process_2018
28	nuclear-transcribed mRNA catabolic process (GO:0000956)	17/175	6.9899324550	0.0003963291	0	0	4.19623573	59.4758706	RPS7;RPS5;F	GO_Biological_Process_2018
29	peptide biosynthetic process (GO:0043043)	17/175	6.9899324550	0.0003566962	0	0	4.19623573	59.4758706	RPS7;MRPS2	GO_Biological_Process_2018
30	rRNA metabolic process (GO:0016072)	18/201	1.0939569396	0.0005074965	0	0	3.86834725	53.0958095	UTP15;RPS7;	GO_Biological_Process_2018
31	rRNA processing (GO:0006364)	18/203	1.2630718406	0.0005371213	0	0	3.83023545	52.0221194	UTP15;RPS7;	GO_Biological_Process_2018
32	translation (GO:0006412)	19/233	2.2650960072	0.0008891373	0	0	3.52246498	45.7846244	MRPS24;RPS	GO_Biological_Process_2018
33	viral process (GO:0016032)	18/221	4.2461156389	0.0015477091	0	0	3.51827057	43.5192688	RANBP2;RPS	GO_Biological_Process_2018
34	mitochondrial ATP synthesis coupled electron transport (GO:004277	11/86	4.6602675568	0.0015854230	0	0	5.52513938	67.8290294	NDUFA13;ND	GO_Biological_Process_2018
35	ribosome biogenesis (GO:0042254)	18/227	6.1737508478	0.0019690406	0	0	3.42527664	41.086892	UTP15;RPS7;	GO_Biological_Process_2018
36	ncRNA processing (GO:0034470)	18/228	6.5623672682	0.0019698682	0	0	3.4102535	40.698508	UTP15;RPS7;	GO_Biological_Process_2018
37	respiratory electron transport chain (GO:0022904)	11/95	1.2341294187	0.0034987569	0	0	5.00170513	56.5320706	NDUFA13;ND	GO_Biological_Process_2018
38	gene expression (GO:0010467)	24/412	3.6661542004	0.0098465183	0	0	2.51630355	25.7009765	RANBP2;RPS	GO_Biological_Process_2018
39	fatty acid oxidation (GO:0019395)	7/51	0.0001634500	0.0417042818	0	0	5.92893745	51.6944239	ACADL;ECI1;	GO_Biological_Process_2018
40	fatty acid beta-oxidation (GO:0006635)	7/51	0.0001634500	0.0397183636	0	0	5.92893745	51.6944239	ACADL;ECI1;	GO_Biological_Process_2018
41	ribosome (GO:0005840)	14/77	2.3166517915	1.0332266990	0	0	7.85391714	156.160557	RPS7;DHX9;F	GO_Cellular_Component_2018
42	cytosolic ribosome (GO:0022626)	16/125	3.2420827636	7.2298445629	0	0	5.52915767	95.3473647	RPS7;RPS5;F	GO_Cellular_Component_2018
43	polysomal ribosome (GO:0042788)	8/29	2.1739502116	3.2319393146	0	0	11.9162881	182.814327	RPL7A;DHX9	GO_Cellular_Component_2018
44	cytosolic part (GO:0044445)	16/160	1.0068540108	0.0001122642	0	0	4.31965443	59.6487254	RPS7;RPS5;F	GO_Cellular_Component_2018
45	polysome (GO:0005844)	10/64	1.9857457595	0.0001771285	0	0	6.74946004	88.6171437	RPL7A;DHX9	GO_Cellular_Component_2018
46	cytosolic small ribosomal subunit (GO:0022627)	8/50	1.7758618489	0.0013200573	0	0	6.91144708	75.6018288	RPS27;RPS7	GO_Cellular_Component_2018
47	small ribosomal subunit (GO:0015935)	8/54	3.1741224241	0.0020223694	0	0	6.39948804	66.2852205	RPS27;RPS7	GO_Cellular_Component_2018
48	cytosolic large ribosomal subunit (GO:0022625)	8/70	0.0002085490	0.0116266070	0	0	4.93674792	41.8405998	RPL7A;RPLP(	GO_Cellular_Component_2018
49	large ribosomal subunit (GO:0015934)	8/73	0.0002795591	0.0138537081	0	0	4.73386787	38.7339115	RPL7A;RPLP(	GO_Cellular_Component_2018
50	ficolin-1-rich granule lumen (GO:1904813)	10/124	0.0006237135	0.0278176225	0	0	3.48359228	25.7082819	EEF1A1;ALAI	GO_Cellular_Component_2018
51	endocytic vesicle lumen (GO:0071682)	4/18	0.0006702942	0.0271773869	0	0	9.59923206	70.1492075	SPARC;HBB;/	GO_Cellular_Component_2018
52	mitochondrial inner membrane (GO:0005743)	18/342	0.0011028826	0.0409904699	0	0	2.27350233	15.4821598	NDUFA13;ND	GO_Cellular_Component_2018
53	RNA binding (GO:0003723)	56/1388	3.4592110509	0.0398155191	0	0	1.74280006	17.9018416	OTUD4;CELF	GO_Molecular_Function_2018
54	RNA polymerase binding (GO:0070063)	5/19	5.7845249375	0.0332899410	0	0	11.3675117	110.921214	ZFP36;DHX9;	GO_Molecular_Function_2018
55	Cytoplasmic Ribosomal Proteins WP163	15/92	3.0072409788	5.2927441227	0	0	7.04291483	138.197785	RPS7;RPS5;F	WikiPathways_2019_Mouse
56	Fatty Acid Beta Oxidation WP1269	7/34	1.0660091045	0.0009380880	0	0	8.89340617	101.820639	ACADL;GK;E(	WikiPathways_2019_Mouse
57	Mitochondrial LC-Fatty Acid Beta-Oxidation WP401	5/16	2.3013966424	0.0013501526	0	0	13.4989201	144.160493	ACADL;ECI1;	WikiPathways_2019_Mouse
58	mRNA processing WP310	22/457	0.0010577431	0.0465406987	0	0	2.07948353	14.2478263	RNASEH2A;F	WikiPathways_2019_Mouse
59	Fatty acid oxidation WP2318	3/10	0.0013102260	0.0461199575	0	0	12.9589633	86.0158391	ACADM;HADI	WikiPathways_2019_Mouse